C.P. No. 214
(17,183)
A.R C. Technical Report

C.P. No. 214
(17,183)
A.R C. Technical Report

MINISTRY OF SUPPLY

AERONAUTICAL RESEARCH COUNCIL

CURRENT PAPERS

The Laminar Boundary-layer with Distributed Suction on an Infinite Yawed Cylinder

By

K. D. P. Sinha, M.Sc.,

(Engineering Laboratory, Cambridge)

Communicated by Prof. W. A. Mair

LONDON : HER MAJESTY'S STATIONERY OFFICE

1956

FOUR SHILLINGS NET

C.P. No. 214

The Laminar Boundary-layer with Distributed Suction on an Infinite Yawed Cylinder

- By -
K. D. P. Sinha, M.Sc.,
(Engineering Laboratory, Cambridge)

Communicated by Prof. W. A. Mair

11th November, 1954

Summary

Rott and Crabtree have considered the chordwise boundary-layer flow on a yawed infinite cylinder with chordwise stream velocity $U = c\,x^m$, (x is the co-ordinate in the chordwise direction). They showed that this yields 'similar' velocity distributions, and when there is no suction, the spanwise velocity profiles are approximately coincident with the exact Blasius profile, on a scale determined by the ratio of the normal co-ordinate to the momentum thickness. This phenomenon has been further examined, and an explanation of it is given.

The work has been further extended to the case of distributed suction; and numerical solutions have been obtained for the spanwise flow for those cases for which the chordwise solutions were available. The velocity distributions are presented in tables and graphs. It is shown that with distributed suction the spanwise profiles also form universal systems, one system for each distribution of suction, the representative profile being the one for zero pressure-gradient and the corresponding suction.

Besides numerical solutions, an exact analytic solution of the spanwise flow has been obtained for the chordwise stream velocity $U = c\,x^{-1/3}$, and velocity distributions for different suction distributions are given.

Another exact solution obtained refers to the spanwise flow for the chordwise stream velocity $U = c/x$. This is the well-known asymptotic suction profile, for which the ratio of the displacement thickness to the momentum thickness is found analytically to be 2.0.

Further, it has been observed from earlier results that the momentum thickness and displacement thickness decrease with increasing suction and also with decreasing positive pressure-gradients. It is shown here that the ratio of the displacement thickness to the momentum thickness decreases with increasing suction and is nearly independent of the pressure gradient for any given suction. For large suctions, the variation of the above ratio is small enough to be ignored for all practical purposes.

Finally, the behaviour of the spanwise flow in the boundary layer is compared with the chordwise flow, and certain conclusions are drawn for varying pressure-gradients.

Contents/

Contents

1./

1. Introduction

The boundary-layer flow over an infinite yawed cylinder is of considerable interest, because many modern aircraft have swept-back wings. It is well-known that for the infinite yawed cylinder, the laminar boundary-layer equations separate, and it becomes evident that laminar chordwise flow is independent of the spanwise flow. The fact has been supported by the experimental observations of A. D. Young and T. B. Booth[1] in their work on the profile drag of infinite yawed wings. But the spanwise flow can only be computed if the chordwise solution has been given.

W. R. Sears[2] has considered the spanwise flow for zero pressure-gradient in the chordwise direction, and has shown that in this case both the chordwise and spanwise velocity profiles are the exact Blasius' profile. He has also concluded that in this case the boundary-layer remains unaffected by the yaw of the leading edge, and the flow at all points is in the direction of the free-stream.

J. C. Cooke[3] has considered the case when the chordwise velocity distribution at the edge of the boundary layer is of the form $U = cx^m$; which yields 'similar' profiles for the chordwise flow. Making use of Hartree's solutions[4] for the unyawed wing he has computed the spanwise velocity profiles for the range of β covered by Hartree.

The absence of any pressure-gradient term in the spanwise flow equation led Rott and Crabtree[5] to suggest that the spanwise profiles are of similar shapes. They made use of Cooke's solutions in the development of an approximate method for the case of an arbitrary chordwise velocity distribution at the edge of the boundary layer; and found that Cooke's spanwise profiles, when plotted against z/θ_y, lay very close together and approximated closely to the Blasius' profile. An explanation of this observation is sought in the present paper, and it is also found that even better agreement with the Blasius' profile can be obtained, if the velocity ratio is plotted against z/δ_y^*.

In view of the possible practical applications of boundary-layer control by suction, to swept-wing aircraft, the calculations have been extended in the present paper to include a range of values of distributed suction, and the spanwise profiles have been obtained. For these calculations, use was made of the chordwise profiles that were available from the solutions of two-dimensional flow with distributed suction, an account of which is given below.

The solution to the simplest problem of flow over a flat plate, when the suction velocity is proportional to x^{-2}, was first obtained by Schlichting and Bussmann[6]. The same problem was considered by Preston[7], and on his suggestion Thwaites[8] computed the solutions on a differential analyser for a number of suction-parameters. An approximate solution has also been obtained by Watson and Preston[9] using the Piercy-Preston iteration method. Its interest is mainly academic but suggestions for practical applications have been made by Preston and Thwaites.

The solution for another important case of stagnation flow with constant suction was obtained by Schlichting and Bussmann[6]. This case is of significance, because the suction velocity becomes constant and the condition can be made practical by applying suction from the front stagnation point of a wing over a part or whole of the chord.

To the knowledge of the author, no other solution for positive m or β is known.

A/

A large number of solutions for negative values of m (or β) has been obtained by Thwaites[10] by relaxation methods, and exact solutions for the cases $m = -1/3$ (or $\beta = -1$) and $m = -1$ (or $\beta = -\infty$) have also been obtained.

In the present paper the author has considered the spanwise flow for the cases given above and has also carried out an analysis of the spanwise profiles for different suction-distributions.

2. Notation

x, y, z	co-ordinates measured in the chordwise direction, spanwise direction, and normal to the surface respectively.
u, v, w	velocity components in x, y, z directions respectively.
U	Chordwise velocity at the edge of the boundary layer.
V_o	spanwise velocity in the free-stream
p	static pressure in the boundary layer
w_o	normal suction velocity at the surface
ψ	stream function
η	a non-dimensional quantity $= \left(\frac{U}{\nu x}\right)^{\frac{1}{2}} z$
ν	kinematic viscosity $= \mu/\rho$
m	index in the relation
$f(\eta)$	a function defined by $\psi = (\nu U x)^{\frac{1}{2}} f(\eta)$
$f'(\eta) = \frac{u}{U} =$	non-dimensional chordwise velocity
Y	a non-dimensional quantity $= [\frac{1}{2}(m+1)]^{\frac{1}{2}} \eta$
β	semi-wedge angle $= \frac{2m}{1+m}$
$F(Y) =$	$[\frac{1}{2}(m+1)]^{\frac{1}{2}} f(\eta)$
$K = F_0 =$	value of $F(Y)$ on the surface
$g'(\eta) = G'(Y) = \frac{v}{V_o} =$	non-dimensional spanwise velocity constants
α	angle in radians given by $K = \sqrt{2} \cosh \alpha$
Z	a variable given by $Z = \frac{Y}{\sqrt{2}} + \sinh \alpha$

$G_1(Z)/$

$G_1(Z)$ a function given by $F(Y) = \sqrt{2}\, G_1(Z)$

J a function given by $G_1 - Z = 1/J$

g an integer denoting step of integration

$$G_2'(Z) = G'(Y) = \frac{v}{V_o}$$

$$\phi(Y) = \int_{\sigma}^{Y} F\,dY$$

$$X(Y) = e^{-\phi(Y)}$$

$$E(Y) = \int_{o}^{Y} X\,dY$$

$$S(Y) = 1 - G'(Y)$$

$$M(Y) = G'(1 - G')$$

δ_y^* spanwise displacement thickness

θ_y spanwise momentum thickness

$$H_y = \frac{\delta_y^*}{\theta_y}, \quad \Phi_x = \theta_x\left[\tfrac{1}{2}(m+1)\right]^{\frac{1}{2}}\left(\frac{U}{\nu x}\right)^{\frac{1}{2}}, \quad \Phi_y = \theta_y\left[\tfrac{1}{2}(m+1)\right]^{\frac{1}{2}}\left(\frac{U}{\nu x}\right)^{\frac{1}{2}}$$

$$\Delta^x = \delta_x^*\left[\tfrac{1}{2}(m+1)\right]^{\frac{1}{2}}\left(\frac{U}{\nu x}\right)^{\frac{1}{2}}, \quad \Delta^y = \delta_y^*\left[\tfrac{1}{2}(m+1)\right]^{\frac{1}{2}}\left(\frac{U}{\nu x}\right)^{\frac{1}{2}}$$

δ^n central differences of order n

$t(Y) = \int_{o}^{Y} t'\,dY$, a general function

3. Theory and Analysis

The boundary layer equations for the laminar flow over an infinite yawed cylinder are

$$u\frac{\partial u}{\partial x} + w\frac{\partial u}{\partial z} = -\frac{1}{\rho}\frac{\partial p}{\partial x} + \nu\frac{\partial^2 u}{\partial z^2}, \qquad \ldots(1)$$

$$u\frac{\partial v}{\partial x} + w\frac{\partial v}{\partial z} = \nu\frac{\partial^2 v}{\partial z^2}, \qquad \ldots(2)$$

$$\frac{\partial p}{\partial z} = 0, \qquad \ldots(3)$$

and the equation for continuity is

$$\frac{\partial u}{\partial x} + \frac{\partial w}{\partial z} = 0. \qquad \ldots(4)$$

This/

This allows the use of the stream-function ψ for which

$$u = \frac{\partial \psi}{\partial z} \quad \text{and} \quad w = -\frac{\partial \psi}{\partial x}.$$

The boundary conditions are:-

(a) at the surface, $z = 0$, $u = v = 0$,

and $w = w_o$ is zero or non-zero according as the boundary is solid or porous, and

(b) at the edge of the boundary layer

$$z \to \infty, \quad u = U, \quad v = V$$

$$\frac{\partial u}{\partial z} = \frac{\partial v}{\partial z} = \frac{\partial^2 u}{\partial z^2} = \frac{\partial^2 v}{\partial z^2} = 0.$$

If the flow outside the boundary layer is irrotational

$$\frac{\partial U}{\partial y} - \frac{\partial V}{\partial x} = 0. \qquad \ldots(5)$$

Since the cylinder being infinite in length, $\frac{\partial U}{\partial y} = 0$,

so that V = constant = V_o (say). Using equation (3) and the boundary condition at the edge of the boundary layer, equation (1) gives

$$U \frac{dU}{dx} = -\frac{1}{\rho} \frac{\partial p}{\partial x}. \qquad \ldots(6)$$

Applying the well-known transformation

$$\psi = (\nu U x)^{\frac{1}{2}} f(\eta), \quad \eta = \left(\frac{U}{\nu x}\right)^{\frac{1}{2}} z,$$

and using the velocity distribution $U = cx^m$, equation (1) reduces to

$$f''' + \tfrac{1}{2}(m+1) ff'' = m[(f')^2 - 1], \qquad \ldots(7)$$

where

$$f'(\eta) = \frac{u}{U},$$

and

$$w = -\tfrac{1}{2}\left(\frac{U\nu}{x}\right)^{\frac{1}{2}} [(m+1) f + (m-1) \eta f']. \qquad \ldots(8)$$

This is the well-known equation obtained by Falkner and Skan[11].

The/

The boundary conditions are

$$f'(0) = 0$$

and $f(0)$ is zero or non-zero according as the boundary is solid or porous, and

$$f'(\infty) = 1.$$

Hartree[4] used the transformation

$$\left.\begin{aligned} Y &= \sqrt{\frac{m+1}{2}}\,\eta \\ F(Y) &= \sqrt{\frac{m+1}{2}}\,f(\eta), \\ \beta &= \frac{2m}{m+1}, \end{aligned}\right\} \qquad \ldots(9)$$

and considered equation (7) in the form

$$F''' + FF'' = \beta[(F')^2-1], \qquad \ldots(10)$$

with the boundary conditions:-

$$F'(0) = 0,$$

$$F(0) = \text{zero},$$

$$F'(\infty) = 1.$$

He tabulated the solutions partly by direct computation and partly on a differential analyser for a series of values of β, and found that values of β less than -0.1988 will not yield velocity distributions, which satisfy the boundary conditions.

For flow with suction the conditions $F'(0) = 0$ and $F'(\infty) = 1$ are essential, but if $F(0) = K$, then from (8) and (9), the suction velocity at the surface is given by

$$w_o = -K\sqrt{\frac{m+1}{2}} \cdot \left(\frac{U\nu}{x}\right)^{\frac{1}{2}}. \qquad \ldots(11)$$

The solutions of equation (10) with suction are the chordwise solutions and have been described in the introduction for different cases.

Using the same expressions for ψ and η, and taking $g'(\eta) = \frac{v}{V_o}$, the equation (2) reduces to

$$g''' + \tfrac{1}{2}(m+1)\,fg'' = 0, \qquad \ldots(12)$$

with boundary conditions $g'(0) = 0$, $g'(\infty) = 1$, and the condition for $f(0)$ the same as in the chordwise flow. Using Hartree's transformation (9), and taking $g'(\eta) = G'(Y)$, the equation (12) reduces to

$$G''' + FG'' = 0, \qquad \ldots(13)$$

with/

with the boundary conditions:

$$G'(0) = 0, \quad F(0) = K, \quad G'(\infty) = 1.$$

Cooke[3] has studied the case for $K = 0$ and has given solutions which were based on Hartree's solutions.

The solutions for different values of K and β are considered in the present paper.

3.1 Zero-suction Case

No theory is given for this case as this has been dealt with by Cooke[3], and the results of Rott and Crabtree[5] will be discussed later on.

3.2 Suction Case

(a) m (or β) $= 0$: In this case the chordwise velocity at the edge of the boundary layer becomes $U = c =$ constant, and the pressure gradient is zero. The equation for chordwise flow reduces (putting $m = 0$ in (7)) to

$$f''' + \tfrac{1}{2} ff'' = 0, \qquad \ldots(14)$$

with the boundary conditions

$$f'(0) = 0, \quad f(0) = \sqrt{2}\,K, \text{ and } f'(\infty) = 1.$$

The equation was studied and solved by Thwaites[8] for different values of K, although in his case the equation was slightly different in form. The solution is

$$\frac{u}{U} = f' = c_1 \int_0^{\eta} e^{-\frac{1}{2}\int f d\eta}\, d\eta,$$

where c_1 is determined by the boundary condition $f'(\infty) = 1$, thus giving the solution as

$$\frac{u}{U} = f' = \frac{\int_0^{\eta} e^{-\frac{1}{2}\int f d\eta}\, d\eta}{\int_0^{\infty} e^{-\frac{1}{2}\int f d\eta}\, d\eta}. \qquad \ldots(15)$$

The corresponding spanwise equation reduces to

$$g''' + \tfrac{1}{2} fg'' = 0, \qquad \ldots(16)$$

with the boundary conditions $g'(0) = 0$, $g'(\infty) = 1$, and $f(0) = \sqrt{2}\,K$.

The solution of (16) is easily seen to be

$$\frac{v}{V_c} = g' = \frac{\int_0^{\eta} e^{-\frac{1}{2}\int f d\eta}\, d\eta}{\int_0^{\infty} e^{-\frac{1}{2}\int f d\eta}\, d\eta}, \qquad \ldots(17)$$

the constant of integration being evaluated from the boundary condition $g'(\infty) = 1$.

The/

The solutions (15) and (17) are identical, and thus the equation (16) is taken to be solved, because (14) has already been solved by Thwaites[8].

(b) Stagnation Flow ($m = 1$): In this case, putting $m = 1$ in (7), the chordwise flow equation becomes

$$f''' + ff'' = (f')^2 - 1, \qquad \ldots(18)$$

with the boundary conditions: $f'(0) = 0$, $f(0) = -\dfrac{w_o}{(c\nu)^{\frac{1}{2}}} = K$, and $f'(\infty) = 1$. This equation was studied and solved by Schlichting and Bussmann[6].

The corresponding spanwise flow equation, obtained by putting $m = 1$ in (12), reduces to

$$g''' + f\,g'' = 0, \qquad \ldots(19)$$

with the boundary conditions:

$$g'(0) = 0, \quad f(0) = \text{constant} = K$$

and $$g'(\infty) = 1.$$

The solution of (19), is

$$\frac{v}{V_o} = g' = \frac{\int_o^{\eta} e^{-\int f d\eta}\, d\eta}{\int_o^{\infty} e^{-\int f d\eta}\, d\eta}. \qquad \ldots(20)$$

The spanwise velocity profiles have been obtained by numerical integration of (20).

(c) General Case (m positive or negative): In this case the chordwise equation will be given by (10), which has been discussed before.

The corresponding spanwise-flow equation, from (13), is given by

$$G''' + F\,G'' = 0, \qquad \ldots(21)$$

with the boundary conditions:

$$F(0) = K, \quad G'(0) = 0, \quad G'(\infty) = 1,$$

and the solution of (21) is

$$\frac{v}{V_o} = G'(Y) = \frac{\int_o^{Y} e^{-\int F dY}\, dY}{\int_o^{\infty} e^{-\int F dY}\, dY}, \qquad \ldots(22)$$

the constant of integration being evaluated from the boundary condition $G'(\infty) = 1$. The velocity profiles are obtained in the present paper by numerical methods of integration for those cases for which chordwise solutions are available.

(d)/

(d) Special Case of $m = -1/3$ or $\beta = -1$: In this case the chordwise flow equation is obtained from (10) as

$$F''' + FF'' = -[(F')^2 - 1], \qquad \ldots(23)$$

with the same boundary conditions, and after integrating twice the result is

$$F' + \tfrac{1}{2}F^2 = \tfrac{1}{2}Y^2 + AY + \tfrac{1}{2}K^2, \qquad \ldots(24)$$

where A is a constant of integration and the other constant has been evaluated by the condition $Y = 0$ in (24).

Thwaites[12] has studied the values of the constant 'A' and has found, that for a valid physical solution, the suction velocity must not be less than that given by $K = \sqrt{2}$.

(i) Thwaites' Exact Solution for the Chordwise Flow: Using Thwaites'[12] transformation in which he defines α, Z, and G_1 by

$$\left.\begin{aligned} K &= \sqrt{2}\cosh\alpha \\ Z &= \frac{Y}{\sqrt{2}} + \sinh\alpha \\ F(Y) &= \sqrt{2}\,G_1(Z) \end{aligned}\right\} \qquad \ldots(25)$$

equation (24) reduces to

$$G_1' + G_1^2 = Z^2 + 1, \qquad \ldots(26)$$

and, putting $G_1 - Z = \frac{1}{J}$, this in turn becomes

$$J' - 2ZJ = 1, \qquad \ldots(27)$$

the solution of which is

$$J = \frac{\sqrt{\pi}}{2} e^{Z^2} [\operatorname{erf} Z + B] \qquad \ldots(28)$$

where,

$$B = \frac{2}{\sqrt{\pi}} e^{\alpha - \sinh^2\alpha} - \operatorname{erf}(\sinh\alpha). \qquad \ldots(29)$$

This is evaluated by the boundary condition on the surface

$$\left.\begin{aligned} Y = 0,\ Z = \sinh\alpha,\ F(0) &= \sqrt{2}\cosh\alpha \\ G_1(\sinh\alpha) &= \cosh\alpha \\ J(\sinh\alpha) &= e^{\alpha} \end{aligned}\right\}. \qquad \ldots(30)$$

Making/

Making reverse substitutions, Thwaites[12] has obtained the exact solution given by

$$\frac{u}{U} = F'(Y) = 1 - \frac{4}{\sqrt{\pi}} \cdot e^{-\left(\frac{Y}{\sqrt{2}}+\sinh\alpha\right)^2} \times \frac{N}{D}, \qquad \ldots(31)$$

where

$$N = \left[\left\{\operatorname{erf}\left(\frac{Y}{\sqrt{2}} + \sinh\alpha\right) + B\right\}\left\{\frac{Y}{\sqrt{2}} + \sinh\alpha\right\} + \frac{1}{\sqrt{\pi}} \cdot e^{-\left(\frac{Y}{\sqrt{2}}+\sinh\alpha\right)^2}\right],$$

and

$$D = \left[\operatorname{erf}\left(\frac{Y}{\sqrt{2}} + \sinh\alpha\right) + B\right]^2.$$

The corresponding exact solution for the spanwise flow is given below.

(ii) The Exact Solution for the Spanwise Flow: From equation (21), the spanwise flow is given by

$$G''' + F\,G'' = 0, \qquad \ldots(32)$$

with the boundary conditions:

$$G'(0) = 0, \quad F(0) = K, \quad G'(\infty) = 1.$$

Using the transformation (25), and putting $G'(Y) = G_2'(Z)$, the above equation reduces to

$$G_2''' + 2\,G_1 G_2'' = 0, \qquad \ldots(33)$$

with the boundary conditions:

$$\left.\begin{array}{lll} Z = \sinh\alpha, & G_1(\sinh\alpha) = \dfrac{K}{\sqrt{2}} & \\ & G_2'(\sinh\alpha) = 0 & \\ Z = \infty & G_2'(\infty) = 1 & \end{array}\right\}, \qquad \ldots(34)$$

where dashes denote differentiations with respect to Z.

The solution of (33) is given by

$$G_2'(Z) = \frac{\displaystyle\int_{\sinh\alpha}^{Z} e^{-\int_{\sinh\alpha}^{Z} 2\,G_1\,dZ}\,dZ}{\displaystyle\int_0^{\infty} e^{-\int_0^{Z} 2\,G_1\,dZ}\,dZ}, \qquad \ldots(35)$$

the constant of integration being found from the condition

$$Z \to \infty, \quad G_2'(\infty) = 1.$$

The/

The numerator of the solution (35) is evaluated as follows.- From (28) and using the relation $G_1(Z) = Z + \frac{1}{J}$, we get

$$G_1 = Z + \frac{2}{\sqrt{\pi}} \cdot \frac{e^{-Z^2}}{(\text{erf } Z + B)}, \qquad \ldots(36)$$

which makes the numerator equal to

$$\int_{\sinh \alpha}^{Z} e^{-Z^2} \cdot e^{-\log(\text{erf } Z + B)^2} \cdot e^{\log \frac{2}{\sqrt{\pi}} e^{\alpha}} \, dZ,$$

since, using (29), $\log (\text{erf } \sinh \alpha + B) + \sinh^2 \alpha = \log \frac{2}{\sqrt{\pi}} e^{\alpha}$.

Integrating further between limits, the numerator becomes

$$e^{\alpha} \left| \frac{1}{\text{erf } \sinh \alpha + B} - \frac{1}{\text{erf } Z + B} \right|. \qquad \ldots(37)$$

The denominator is at once evaluated by making $Z = \infty$ in (37), and using the definite integral $\int_0^{\infty} e^{-t^2} \, dt = \sqrt{\pi}/2$.

Thus the profile is given by

$$\frac{v}{V_o} = G_2'(Z) = \frac{1 - \dfrac{\text{erf } \sinh \alpha + B}{\text{erf } Z + B}}{1 - \dfrac{\text{erf } \sinh \alpha + B}{1 + B}}, \qquad \ldots(38)$$

where B is a constant given before in (29). The boundary conditions are satisfied, since

$$\left.\begin{array}{lllll} Y = 0, & Z = \sinh \alpha, & G_2'(\sinh \alpha) & = & 0 \\ Y = \infty, & Z = \infty, & G_2'(\infty) & = & 1 \end{array}\right\}. \qquad \ldots(39)$$

The error-function has already been tabulated for a large range of the variable, and so from (38), the velocity profiles for different K can be obtained.

As an example, the velocity profile for $K = \sqrt{2}$ is given by

$$\frac{v}{V_o} = \frac{\text{erf } Z}{\text{erf } Z + \frac{2}{\sqrt{\pi}}} \cdot \left(1 + \frac{2}{\sqrt{\pi}} \right), \qquad \ldots(40)$$

since/

since from (25) and (29) $\alpha = 0$, and $B = \frac{2}{\sqrt{\pi}}$ and the boundary conditions are satisfied. When K is large, B decreases to smaller values, and the minimum value of B is -1.

(iii) Case $\beta = -1$: Behaviour when K is very large:- From (38), we have

$$\frac{v}{V_o} = \frac{1 - \dfrac{\text{erf sinh } \alpha + B}{\text{erf } Z + B}}{1 - \dfrac{\text{erf sinh } \alpha + B}{1 + B}},$$

where $$Z = \frac{Y}{\sqrt{2}} + \sinh \alpha, \quad \cosh \alpha = \frac{K}{\sqrt{2}},$$

and $$B = \frac{2}{\sqrt{\pi}} e^{\alpha - \sinh^2 \alpha} - \text{erf}(\sinh \alpha).$$

Putting, $$c_o = \frac{\text{erf sinh } \alpha + B}{1 + B},$$

and using the asymptotic expansion for the error-function we get

$$\frac{v}{V_o} = 1 - \frac{c_o}{1-c_o} T - \frac{c_o}{1-c_o} T^2 - \ldots\ldots\ldots$$

where $$T = \frac{1}{\sqrt{\pi}(1+B)} \cdot \frac{e^{-Z^2}}{Z} \left(1 - \frac{1}{2Z^2} + \frac{3}{4Z^4} - \ldots\ldots\ldots \right).$$

Also, using the expansion

$$\sinh \alpha = \frac{K}{\sqrt{2}} \left[1 - \frac{1}{K^2} - \frac{1}{2K^4} + \ldots\ldots \right],$$

and neglecting quantities of $O(1/K^3)$ and higher orders, we get

$$\text{erf sinh } \alpha = 1 - \frac{\sqrt{2}\, e}{\sqrt{\pi}} \cdot \frac{e^{-K^2/2}}{K},$$

and $$B = \frac{2\sqrt{2}\, e\, K}{\sqrt{\pi}} e^{-K^2/2} - 1.$$

Then, replacing Z in terms of ζ and making similar approximations, the velocity ratio becomes

$$\frac{v}{V_o} = 1 - e^{-\zeta} + \frac{e^{-\zeta}}{2K^2} \left(1 + \zeta^2 - e^{-\zeta} \right) + O\left(\frac{1}{K^4} \right).$$

Again/

Again, making calculations for displacement thickness and momentum thickness, we get

$$\frac{-\delta_y^* w_o}{\nu} = 1 + O\left(\frac{1}{K^2}\right),$$

and

$$\frac{-\theta_y w_o}{\nu} = \frac{1}{2} + O\left(\frac{1}{K^2}\right).$$

When, $K \to \infty$, $v/V_o \to 1 - e^{-\zeta}$, and $H_y = \frac{\delta_y^*}{\theta_y} \to 2$, which is the asymptotic suction case for the spanwise flow.

(e) The Case of $m = -1$ (or $\beta = -\infty$): In this case $U = c/x$, and $F(Y) = \sqrt{\frac{m+1}{2}}\, f(\eta)$ (Hartree's transformation) and there is a failure of the equations (10) and (21). Thwaites[12] has suggested another transformation, when dealing with the two-dimensional flow with distributed suction, and has given an exact solution for this case, which serves as the solution for chordwise flow over infinite yawed cylinder.

(i) Thwaites' Chordwise Solution: Using Thwaites' transformation

$$\left.\begin{aligned} \psi &= \sqrt{\nu U x}\,[f(\eta) + K \log x], \\ \eta &= \left(\frac{U}{\nu x}\right)^{\frac{1}{2}} z, \end{aligned}\right\} \qquad \ldots(41)$$

we get $u = U f'(\eta)$, $w = \sqrt{c\nu}\left[\frac{\eta}{x} f' - \frac{K}{x}\right]$,

and the chordwise flow equation reduces to

$$f''' + K f'' = 1 - (f')^2, \qquad \ldots(42)$$

which was obtained and solved by Thwaites[12].

It is worth remarking that with $K = 0$, and $f'(\infty) = 1$, Pohlhausen's solution[13] for convergent flow between solid walls is obtained, which is one of the few known exact solutions.

In the solution of (42) Thwaites[12] has made an analysis for K and has found that for physical validity K must be greater than or equal to $\sqrt{8}$.

(ii) The Exact Solution for Spanwise Flow: Using the transformation (41), and taking $g'(\eta) = \frac{v}{V_o}$, the equation of motion for spanwise flow becomes

$$g''' + K g'' = 0, \qquad \ldots(43)$$

with/

with the boundary conditions $g'(0) = 0$ and $g'(\infty) = 1$. The solution of (43) is given by

$$\frac{v}{V_o} = g'(\eta) = 1 - e^{-K\eta}, \qquad \ldots(44)$$

the constants of integration being evaluated by the two boundary conditions.

Calculating other boundary layer quantities, we get,

$$\theta_y = \int_o^\infty \frac{v}{V_o}\left(1 - \frac{v}{V_o}\right) dz = \frac{1}{2K} \cdot x\left(\frac{\nu}{c}\right)^{\frac{1}{2}}, \qquad \ldots(45)$$

$$\delta_y^* = \int_o^\infty \left(1 - \frac{v}{V_o}\right) dz = \frac{1}{K} x\left(\frac{\nu}{c}\right)^{\frac{1}{2}}, \qquad \ldots(46)$$

and

$$H_y = \frac{\delta_y^*}{\theta_y} = 2. \qquad \ldots(47)$$

The solution (44) can be written in the form

$$\frac{v}{V_o} = g'(\eta) = 1 - e^{-\frac{1}{2}(z/\theta_y)}, \qquad \ldots(48)$$

since $z/\theta_y = 2K\eta$.

The solution (48) is the well known asymptotic suction profile and is independent of K.

4. Numerical Methods of Solutions and Computations

Besides giving exact solutions for the spanwise flow over an infinite yawed cylinder for the cases $m = 0$, $m = -1/3$ and $m = -1$, a number of results have been obtained by numerical methods and rather laborious computations. The numerical solution for each velocity profile consisted of three integrations, and the calculations involved the use of a large number of derivatives on the surface of the boundary, and preparations of three charts of 'finite differences', one necessary for each integration. The 'finite differences' used here are the 'central differences'[14], and these have the advantage that they exist alternately and good accuracy is obtained by including only few orders. The method was found to be convenient in one more respect, that the derivatives at the edge of the boundary layer vanished, and made the calculations simpler. Momentum thickness and displacement thickness were also calculated by these numerical methods. The calculations are not given here in detail, and only the important steps are indicated.

The general solution for the velocity profile is given by

$$\frac{v}{V_o} = G'(Y) = \frac{\int_o^Y e^{-\int F dY}\, dY}{\int_o^\infty e^{-\int F dY}\, dY}, \qquad \ldots(49)$$

and/

and its evaluation is carried out in four parts, viz.,

(a) calculation of F from chordwise solution

(b) calculation of $\phi(Y) = \int_0^Y F dY$,

(c) calculation of $E(Y) = \int_0^Y e^{-\phi(Y)}\, dY = \int_0^Y X(Y) dY$,

and (d) calculation of the constant $\int_0^\infty X\, dY$.

The formula used for the step-by-step integration is

$$\int_{Y_g^\bullet - 1}^{Y_g^\bullet} t' dY = t_g^\bullet - t_g^\bullet - 1 = \frac{\delta Y}{2}\left[t'^\bullet_g + t'^\bullet_g - 1 - \frac{1}{12}\left(\delta^2 t'^\bullet_g + \delta^2 t'^\bullet_g - 1 \right) + \frac{11}{720}\left(\delta^4 t'^\bullet_g + \delta^4 t'^\bullet_g - 1 \right)\right], \qquad \ldots(50)$$

maintaining 'central differences' only up to the fourth order. The 'central differences' on the surface are calculated by the formulas

$$\delta^2 t'_o = (\delta Y)^2 \left[t'''_o + \frac{(\delta Y)^2}{12} t^{v}_o + \frac{1}{360}(\delta Y)^4 t^{vi}_o \right],$$

and

$$\delta^4 t'_o = (\delta Y)^4 \left[t^{v}_o + \frac{1}{6}(\delta Y)^2 t^{vii}_o \right], \qquad \ldots(51)$$

neglecting quantities of order greater than $O(\delta Y)^6$. With the aid of formulas (50) and (51), the calculations (a), (b) and (c) can be made.

The constant (d) is evaluated by the formula

$$\int_0^\infty X\, dY = \frac{\delta Y}{2}\left[X_o + X_\eta + 2(X_1 + X_2 + \ldots\ldots + X_{n-1}) - \frac{\delta Y}{6}\left\{ - X'_o + \frac{(\delta Y)^2}{60} X'''_o - \frac{(\delta Y)^4}{2520} X^{v}_o + \frac{(\delta Y)^6}{10080} X^{vii}_o \right\}\right], \qquad \ldots(52)$$

where higher powers of δY are neglected, the boundary conditions at the edge of the boundary layer are used, and n is taken to be infinite by the condition when $G'(Y) = v/V_o = 1$. The derivatives of X''s on the surface are obtained by differentiations of

$$X' + F X = 0. \qquad \ldots(53)$$

The derivatives of F on the surface are obtained by successive differentiations of the main equation (10).

Thus the velocity is calculated by the relation

$$G'^\bullet_g(Y) = c' E^\bullet_g \qquad \ldots(54)$$

where $c' = \dfrac{1}{\int_0^\infty e^{-\int F dY}\, dY}$, and the relation (54) provides a definite

check/

check on the whole calculation, since $E_{co} = 1/c'$ and $G'(\infty) = 1$.

The momentum thickness and displacement thickness are calculated by using formulas like (52) in the forms given by

$$\left(\frac{U}{\nu x}\right)^{\frac{1}{2}}\sqrt{\frac{m+1}{2}}\,\theta_y = \int_0^\infty G'(1-G')\,dY = \int_0^\infty M\,dY, \qquad \text{and} \qquad \left(\frac{U}{\nu x}\right)^{\frac{1}{2}}\sqrt{\frac{m+1}{2}}\,\delta_y^* = \int_0^\infty (1-G')\,dY = \int_0^\infty S\,dY. \qquad \ldots(55)$$

H_y is calculated using the relation $H_y = \dfrac{\delta^*}{\theta_y}$, and the velocity gradient on the surface is calculated by the formula

$$G''(0) = c'. \qquad \ldots(56)$$

The values of F_o, β, and δY are given from the chordwise solutions, and only the corresponding spanwise solutions have been obtained from computations. The method is believed to give good accuracy for all practical purposes, because (i) the coefficients of the series used are rapidly decreasing, (ii) a large number of derivatives calculated from the differentiations of the main differential equations are used for the surface conditions, and (iii) the finite 'central difference' are used up to the fourth order.

Yet, there are two possible sources of errors, which the author has experienced in the process of computation. The first arises from the fact that the interval $\delta Y = 0.5$ as used by Thwaites[10] is rather large, and better results can be expected with a smaller interval. Secondly, with the increasing suction, the derivatives at the boundary increase, and they may also cause some errors for large suctions, but the errors are confined to the fourth decimal place.

5. Discussion of the Results

(a) Zero-suction Case: No theory is developed for this case as it has already been given by Cooke[3], and the author has examined the property of the spanwise profiles noted by Rott and Crabtree[5]. As mentioned before, they discovered that all the spanwise velocity profiles, if plotted against z/θ_y, lie very close together and they all approximate to the exact Blasius' profile. The present author further obtained the graphs of the spanwise velocity ratio against two other boundary-layer quantities, viz., (1) η and (2) against z/δ_y^*.

In the former case, the profiles were of the same shape but did not coincide. A graphical transformation for η was attempted with a view to bringing the profiles nearer to coincidence with the exact Blasius' profile, and after finding suitable factors for η with the help of Blasius' profile, all the spanwise profiles lay very close together and approximated to the exact Blasius' profile. (The profiles are not shown here.)

For the latter case, eight spanwise profiles are plotted, and these are very nearly coincident (Fig.1).

Explanation/

Explanation.- The question arises why it is that the profiles, when plotted against z/θ_y and z/δ^*_y, lie close together and approximate to the Blasius' solution; whereas, when plotted against η, they do not lie together. All the quantities η, z/θ_y and z/δ^*_y are non-dimensional boundary-layer quantities, and the only difference is that η is a function of m, whereas z/θ_y and z/δ^*_y are independent of m. Moreover, by neutralizing the contribution of m to η by choosing suitable factors, the profiles behaved approximately in the desired way. This led the author to show that spanwise profiles plotted against any boundary-layer quantity which is independent of m, will lie very nearly on one curve.

An explanation of the above behaviour of the spanwise profiles is also apparent from the governing equation (equation (13))

$$G''' + F\,G'' = 0,$$

which bears a certain similarity to the Blasius' flow equation

$$f''' + ff'' = 0.$$

A method of solving this given by Watson and Preston[9] was to write it as

$$f_2''' + f_1\,f_2'' = 0,$$

an equation 'similar' to equation (13), where f_1 is a rough approximation to f_2. It turns out that quite different and crude guesses for f_1 yield f_2' - curves satisfying the momentum equation, which are very close to the Blasius' profile. It is seen that, since the F in equation (13) is obtained from the chordwise velocity profiles (F'), G' must be close to the Blasius' profile.

(b) Case of Suction:

(i) $\beta = 0$ (or m = 0): In this case the solutions for the chordwise and spanwise flows coincide, as is evident from (15) and (17). The solutions for chordwise flow for different suction velocities have been given by Thwaites[8], and spanwise profiles based on those solutions are given in Table I.

(ii) Positive Pressure-gradients (β or m negative): For positive pressure-gradients, solutions for chordwise flow have been given by Thwaites[10], and the corresponding solutions for spanwise flow are given in Tables 2 - 6 except for m = - 1/3 and m = - 1. (These two cases will be considered separately.) Five suction values (K = 0.2, 0.4, 0.6, 0.8, 1.0) have been considered and solutions for four values of β have been given for each value of K. Velocity profiles for each value of K have been plotted against z/θ_y, and are shown in Figs. 2 - 6. Other boundary-layer quantities are calculated, and the following conclusions are obtained:-

(a) For each suction value, the profiles for different values of β coincide, and give approximately only one curve when plotted on z/θ_y scale.

(b) The velocity gradient on the surface increases with increasing suction, and also for increasing values of β for each suction.

(c) The displacement thickness decreases with increasing suction; and it also diminishes with increasing values of β for a particular suction.

(d)/

(d) The momentum thickness goes down when the suction quantity goes up, and it also decreases with increasing β for a particular suction.

(e) The values of H_y are nearly the same for a given suction, and the effect of a change of β is negligible.

(f) Examining the values of H_y in the Tables 2 - 8, it is found that H_y decreases with increasing suction, but for large suctions the variation is very small. This led the author to suggest that for very large suctions, H_y can be taken as independent of any suction parameter.

(iii) The Special Cases, $m = -1/3$ and $m = -1$:

(a) The solutions for the case $m = -1/3$ or $\beta = -1$ are given in Table 7, and v/V_o is plotted against z/θ_y in Fig.7, for different suction parameters ($K = 1.414, 1.421, 1.437, 1.50, 1.554$). It is found that all the profiles coincide, and it is suggested that they are nearly independent of suction when plotted on a z/θ_y scale but the suction must be such that $K \geqslant \sqrt{2}$ for physical validity.

The values of displacement thickness and momentum thickness decrease with increasing suction, which is as usual. The values of H_y vary so little with suction (Table 7, Fig.9), they can be taken as constant. This observation supports the statement in 5.(ii) (f) that with very large suctions the variation of H_y is negligible.

(b) The case of $m = -1$ (or $\beta = -\infty$) is the limiting case and is only of theoretical interest. The profile is presented in Table 8 and Fig. 8. It is analytically found to be the well known asymptotic suction profile, and when v/V_o is expressed in terms of z/θ_y, it is independent of K as given in (48). The expressions for displacement thickness and momentum thickness are obtained in (45) and (46) in terms of the suction parameter K. It is interesting to observe that the momentum thickness is half the displacement thickness, i.e., the value of H_y is exactly 2.0. This is the minimum value of H_y for the case of spanwise flow, whereas Thwaites[10] has obtained a smaller value of H in the case of chordwise flow, and the explanation of which is not clear.

(iv) Negative Pressure-gradients (β or m positive): The lack of enough solutions for the chordwise flow prevents the author from discussing this domain fully. The only solution available for this domain is of the stagnation flow ($\beta = 1$) in the chordwise direction given by Schlichting and Bussmann[6]. The corresponding spanwise solution has been obtained, and profiles are given in Table 9 for suction corresponding to $K = 0, 0.5, 1.095, 1.9265$ and 2.664. Other boundary-layer quantities (δ^*_y, θ_y, H_y) have been calculated and are given in the same table.

The velocity ratios are plotted against z/θ_y in Fig. 10, and it is observed that as the suction increases the profiles become nearer and nearer to each other. This fact supports the previous statement that for large suctions the variation in H_y with suction is small, and that for very large suctions the change in the profiles with suction is negligible.

The values of H_y are plotted and in this case also the points lie on the H_y-curve obtained from other solutions for the pressure-rise domain as in Fig.9. This fact indirectly supports the observation, that the profiles based on z/θ_y, for a particular

suction-value/

suction-value and different pressure-gradients are roughly coincident. A direct proof would have been better, but no solution is available for these values of suction-parameter (K 0.5, 1.095, 1.9265 and 2.664) and other values of β (except $\beta = 1$).

As usual, the displacement thickness and the momentum thickness decrease with increasing suction, as will be evident from Table 9.

The value of H_y decreases with increasing suction and tends to 2 - the minimum value of H_y, as is evident from Fig.9 and Table 9.

(v) Universality of Profiles: As has been discussed before, (5.(a)), the spanwise profiles for zero suction form an approximately universal system on a scale which is independent of m, and the representative profile of that system is the one for $m = 0$, which coincides with the exact Blasius' profile.

In case of suction also, a similar idea of a universal system of profiles is contemplated. In the suction case it is clear from the previous discussions, that there cannot be only one universal system of profiles for all suction distributions, but there will be a series of systems of profiles, one for each distribution of suction. The representative profile for each system will be given by the profile for $\beta = 0$ for the corresponding suction. For the verification of this statement, solutions for $\beta = 0$ are required for suctions given by K = 0.2, 0.4, 0.5, 0.6, 0.8, 1.0, 1.095, 1.414, 1.421, 1.437, 1.5, 1.554, 1.9265 and 2.664, but from Table I, only the solution for $\beta = 0$ and K = 1.414 is available for this purpose, and this profile has been plotted in Fig.7 against z/θ_y. It is found from Fig.7 that the profile for $\beta = 0$ coincides with all other profiles for $\beta = -1$, thus verifying the statement made above. It would have been interesting to obtain further verifications, but the solutions are lacking for this purpose.

(vi) Comparison of the Chordwise and Spanwise Flows with Suction: It is not intended here to give a detailed discussion of the similarities and dissimilarities of the chordwise and spanwise flows, but only to point out certain striking features of the two flows connected with this paper. The solutions of the two-dimensional flow given by Thwaites[8,10,12] and Schlichting and Bussmann[6] have been taken for the results of the chordwise flow, and the results for the spanwise flow have been obtained by the author.

The whole discussion is divided into the following sections viz:

(a) $\beta = 0$, (zero-pressure gradient): In the case of zero suction and zero-pressure gradient it has been shown analytically by Sears[2] that the two flows (chordwise and spanwise) have the same Blasius' profile. In the suction case with zero pressure-gradient, the author has shown in 3.2 (a) that the two flows have the same profile for any value of suction-parameter and the solutions have been already given by Thwaites[8] and Schlichting and Bussmann[6] for a number of suction-distributions. Typical chordwise profiles based on z/θ_x have been plotted together with the spanwise profiles in Figs. 2, 3, 4, 5 and 6, and it can be seen that as β tends to zero, the chordwise profile approaches the spanwise profile for $\beta = 0$. It is evident that in this case all other boundary-layer characteristics for the two flows must be the same.

(b)/

(b) $\beta > 0$ (negative pressure-gradients):

(1) In this case the value of F"(0) (wall velocity-gradient for the chordwise flow) is greater than G"(0) (wall velocity-gradient for the spanwise flow), for given values of the suction-parameter and pressure gradient, (i.e., given β)(Fig.13).

(2) It is also found that the momentum thickness and displacement thickness of the chordwise flow are smaller than those of the spanwise flow for given suction and pressure-gradient (Fig.16).

(3) H_x is less than H_y for given suction and pressure-gradient. The value of H_x ranges from 2.218 to 2.077 and H_y changes from 2.5405 to 2.0806 as the suction-parameter K increases from zero to 2.664 (Fig.18) for the case of $\beta = 1$, which is the only solution available for this domain.

These observations suggest that for negative pressure-gradients, the chordwise boundary-layer is thinner than the spanwise one.

(c) $\beta < 0$ (positive pressure-gradients):

(1) In this case G"(0) (the wall velocity-gradient of the spanwise flow) is much greater than F"(0)(the same quantity for chordwise flow), for any given K and β (Figs. 11 and 12).

(2) It is also observed that the momentum thickness and displace-thickness of the spanwise flow are smaller than those of the chordwise flow for the same conditions of suction and pressure-gradient (Figs. 12, 14 and 15).

(3) Again, the value of H_y is always less than H_x in this domain for a given β and K. Moreover the variation of H_x with β is very marked, but that of H_y with β is negligible. Also, the effect of suction on the variation of H_x is more important for all suctions, but the variation of H_y with increasing suction is always small, and for large suctions it is negligible. The maximum value of H_x becomes even greater than 3.8, whereas the maximum value of H_y is never greater than 2.6. Similarly, the minimum value of H_x goes even below 2, but the minimum value of H_y is obtained analytically as 2.0 (Fig.17). For $\beta = -1$, where large suctions are obtained, the value of H_x changes from 3.42 to 2.56, but the variation of H_y is between 2.12 and 2.13, as the suction-parameter increases from 1.414 to 1.554 (Fig.19).

Even for very large suctions with $\beta = -\infty$, the value of H_x varies from 1.905 to 2.025 as K increases from 2.828 to 3.6. This increase of H with K is a unique behaviour. But for the spanwise flow the value of H_y is 2.0, and the profile is the asymptotic suction profile which is independent of K when based on z/θ_y.

It is clear from above illustrations that the variation of H_x with β is marked, but the effect of β on H_y is negligible. Also, the variation of H_x with suction is important even for large suctions and for the asymptotic suction case, but the variation of H_y with K is small and is negligible for large suctions (Figs. 17 and 19).

(4) Separation Phenomenon:- The case of separation arises only in the presence of a positive pressure-gradient, where β is negative. For the purpose of investigating this case the profiles of the spanwise flow have been plotted for values of $(-\beta)$ up to infinity

but/

but they never show any tendency to separation. This can also be seen from the condition $\left(\frac{\partial^2 v}{\partial z^2}\right)_{z=0} = \frac{w_o}{\nu}\left(\frac{\partial v}{\partial z}\right)_{z=0}$, where the righthand side is either negative or zero, since w_o is negative. Moreover, the chordwise profiles plotted in Figs. 2, 3, 4, 5, 6 for large positive pressure-gradients (β = - 0.28, -0.371, -0.474, -0.592, and -0.721) are concave near the wall, and show a tendency to separation. Also, from the arguments of (c) (1), (2) and (3), it is clear that in this case the chordwise boundary-layer is thicker than the spanwise one, and these facts show that separation is purely a phenomenon of the chordwise flow. The same remark was made by R. T. Jones[15].

(5) Asymptotic Suction Profiles:- In the case of β = - 1, both the profiles tend to the asymptotic suction profile as K tends to infinity. The chordwise case was considered by Thwaites[12] and the author has proved the result for the spanwise flow.

For β = $-\infty$, Thwaites[10] has obtained the profiles for certain values of K ranging from 2.828 to 3.6. The corresponding solution for the spanwise flow has been obtained in this report, and it is the simple asymptotic suction profile and is independent of K when based on z/θ_y. This profile is shown in Fig.8 together with chordwise profiles for K 2.828,3, and 3.6 based on z/θ_x. It is important to observe that the chordwise profile for K = 2.828 does not lie on the spanwise asymptotic suction profile, but goes above it. As K increases to 3, the chordwise profile nearly coincides with the asymptotic suction profile, while for K = 3.6, the chordwise profile goes to the right of the asymptotic suction profile as is evident from Fig.10. This behaviour is explained by the fact that for K = 2.828, H_x is 1.905, which is less than 2; while for K = 3, H_x is 1.992, very near to 2, and for K = 3.6, H_x is 2.025, greater than 2 (the value of H_y for the asymptotic suction profile).

From the above discussion, it appears that with still greater suction (K > 3.6), a change in the chordwise flow could be obtained, but the spanwise flow would remain unchanged as the asymptotic suction case with H_y = 2.0.

6. Conclusions

It is shown that all the spanwise profiles for a particular suction approximately coincide when based on a z/θ_y scale, and form a universal system of which the profile for β = 0 is the representative one. It bears an analogy to the case of zero-suction where the exact Blasius' profile is the representative of all the spanwise profiles on the same scale.

Secondly, exact solutions of the spanwise flow for the cases β = - 1 and β = $-\infty$ have been obtained; and in the latter case the solution is the asymptotic suction profile.

Thirdly, it is found that for a particular value of suction-parameters, H_y is very nearly independent of β.

Fourthly, it is shown that H_y decreases with increasing suction, but is never less than 2.0. Also the variation of H_y with suction for very large suctions, is so small, that it can be ignored.

Fifthly,/

Fifthly, it is observed that for zero pressure-gradient, the two boundary-layers are similar; for negative pressure-gradients, the chordwise boundary-layer is thinner than the spanwise one; and for the positive pressure gradients the chordwise boundary-layer is much thicker than the spanwise layer.

Lastly, it is also found that separation is purely a phenomenon of the chordwise flow, and the spanwise profiles never show any tendency to separation.

7. Acknowledgments

I wish to acknowledge the financial help given by the Government of India and the Patna University in the form of a scholarship for my work at Cambridge. I also wish to thank Dr. J. H. Preston who supervised the work; and Professor W. A. Mair and Dr. M. R. Head for their sympathetic interest in the problem.

References

1. Young, A. D. and Booth, T. B.-Profile drag on yawed wings of infinite span. College of Aeronautics Report No.38 (1950).

2. Sears, W. R.- The boundary-layer of yawed cylinders. Journal of Aeronautical Sciences, Vol.15, No.1, January 1948

3. Cooke, J. C.- The boundary-layer of a class of infinite cylinders. Proc. Camb. Phil. Soc., Vol.46, Part 4, October, 1950, p.645.

4. Hartree, D. R.- On an equation occurring in Falkner and Skan's approximate treatment of the equations of the boundary-layer. Proc. Camb. Phil. Soc., Vol.33 (1937), p.223-239.

5. Rott, N. and Crabtree, W. F.- Simplified laminar boundary-layer calculations for bodies of revolution and for yawed wings. Journal of Aeronautical Sciences, Vol.19, No.8, August, 1952.

6. Schlichting, H. and Bussmann, K.- Exakte Lösungen für die Laminare Grenzschicht mit Ausangung und Ausblasen. Sonderdruck aus Band 7B, (1943) Heft 2, der Deutschen Akademie der Luftfahrtforschung.

7. Preston, J. H.- The boundary-layer flow over a permeable surface through which suction is applied. R. & M. 2244. (1946).

8. Thwaites, B.- An exact solution of the boundary-layer equations under particular conditions of porous surface suction. R. & M. 2241. (1946).

9. Watson, E. J. and Preston, J. H.- An approximate solution of two flat plate boundary-layer problems. R. & M. 2537. (1951).

10. Thwaites, B.- The development of laminar boundary layers under conditions of continuous suction. Part II Approximate methods of solution. (8th November, 1949). A.R.C.12,699

11. Falkner and Skan.- Some approximate solutions of the boundary layer equations. R. & M. 1314. (1930).

12./

12. Thwaites, B.- The development of the laminar boundary layer under conditions of continuous suction. Part I On similar profiles. (8th October, 1948). A.R.C.11,830

13. Pohlhausen, K.- Steady two-dimensional convergent flow between solid walls. Zeitschr. f. angene. Math. und Mech. I (1921) 267, 268.

14. Hartree, D. R. Numerical analysis.

15. Jones, R. T.- Effect of sweptback on boundary-layer and separation. N.A.C.A. Technical Note 1402.

APPENDIX

Notes on Table I

This Table I has been prepared from Thwaites' solutions[8] for two-dimensional flow with suction for the case $\beta = 0$. His equation was

$$f''' + ff'' = 0,$$

with the boundary conditions: $f'(0) = 0$, $f'(\infty) = 2$, $f(0) = 2\sigma_1$,

where $\frac{u}{U} = \frac{1}{2} f'(\eta)$, $\psi = (\nu Ux)^{\frac{1}{2}} f$, and $\eta = \frac{1}{2}\left(\frac{U}{\nu x}\right)^{\frac{1}{2}} z$.

Here z has been used instead of y as used by Thwaites[3].

But in the present paper, the equation is

$$f''' + \tfrac{1}{2} ff'' = 0,$$

with the boundary conditions: $f'(0) = 0$, $f'(\infty) = 1$ and $f(0) = \sqrt{2}\,K$,

where $$\frac{u}{U} = f'(\eta) = g'(\eta) = \frac{v}{V_o},$$

$$\eta = \left(\frac{U}{\nu x}\right)^{\frac{1}{2}} z \quad \text{and} \quad \psi = (\nu Ux)^{\frac{1}{2}} f(\eta).$$

The difference is that in the present paper η has twice that in Thwaites' case[8].

The following modifications have been made in preparing Table I from Thwaites' table:-

(i) η is made twice that given in Ref.8

(ii) $\frac{u}{U} = \frac{v}{V_o} = \frac{1}{2} f'(\eta)$, $f'(\eta)$ supplied by Thwaites[8].

(iii) $f(0) = 2\sigma_1$,

(iv) $F_o = \sqrt{2}\,\sigma_1 = K$.

TABLE I/

TABLE I

$\beta = 0$ or $m = 0$

f_o->	1.0	2.0	5.0		10.0		20.0	
η	v/V_o	v/V_o	η	v/V_o	η	v/V_o	η	v/V_o
0	0	0	0	0	0	0	0	0
0.1	0.0705	0.1105	0.05	0.1215	0.0125		0.0125	0.1170
0.2	0.1430	0.2115	0.10	0.2345	0.0250	0.1230	0.0250	0.2215
0.4	0.2685	0.3895	0.15	0.3250	0.0375		0.0375	0.3185
0.6	0.3755	0.5250	0.20	0.4065	0.0500	0.2285	0.0500	0.3995
0.8	0.4765	0.6400	0.30	0.5450	0.0750	0.3155	0.0750	0.5300
1.0	0.5660	0.7300	0.40	0.6550	0.1000	0.3975	0.1000	0.6350
1.2	0.6450	0.8000	0.50	0.7350	0.1250		0.1250	0.7150
1.4	0.7150	0.8550	0.60	0.8000	0.1500	0.5350	0.1500	0.7800
1.6	0.7700	0.8950	0.80	0.8850	0.1750		0.1750	0.8250
1.8	0.8200	0.9250	1.0	0.9350	0.2000	0.6400	0.2000	0.8650
2.0	0.8600	0.9500	1.2	0.9650	0.2500		0.2500	0.9200
2.2	0.8950	0.9650	1.4	0.9800	0.3000	0.7850	0.3000	0.9500
2.4	0.9200	0.9750	1.6	0.9900	0.4000	0.8700	0.4000	0.9800
2.6	0.9400	0.9850	1.8	0.9950	0.5000	0.9250	0.5000	0.9900
2.8	0.9550	0.9900	2.0	0.9950	0.6000	0.9550	0.6000	0.9950
3.0	0.9700	0.9950	2.2	0.9950	0.8000	0.9850	0.8000	1.0000
3.2	0.9800	0.9950	2.4	1.0000	1.0000	0.9950		
3.4	0.9850	1.0000			1.2000	1.0000		
3.6	0.9900							
3.8	0.9950							
4.0	0.9950							
4.2	0.9950							
4.4	1.0000							

TABLE 2/

TABLE 2

$F_o = +0.2$

β →	-0.28		-0.26		-0.20		-0.12	
Y	z/θ_y	v/V_o	z/θ_y	v/V_o	z/θ_y	v/V_o	z/θ_y	v/V_o
0	0	0	0	0	0	0	0	0
0.5	0.914	0.2210	0.997	0.2450	1.089	0.2671	1.141	0.2805
1.0	1.828	0.4201	1.994	0.4636	2.178	0.5028	2.282	0.5258
1.5	2.742	0.5957	2.992	0.6498	3.267	0.6971	3.423	0.7230
2.0	3.656	0.7429	3.989	0.7952	4.356	0.8395	4.564	0.8614
2.5	4.570	0.8554	4.986	0.8963	5.445	0.9283	5.705	0.9422
3.0	5.484	0.9303	5.983	0.9559	6.534	0.9737	6.846	0.9803
3.5	6.398	0.9720	6.980	0.9835	7.624	0.9922	7.987	0.9946
4.0	7.313	0.9910	7.978	0.9948	8.713	0.9981	9.128	0.9987
4.5	8.227	0.9977	8.975	0.9990	9.802	0.9995	10.269	0.9996
5.0	9.141	0.9996	9.972	0.9998	10.891	0.9998	11.410	0.9998
5.5	10.055	1.0	10.969	1.0	11.980	1.0	12.551	1.0
G"(0)	0.4646		0.5157		0.5625		0.5910	
$\int_o^\infty (1-G')dY$	1.3775		1.2478		1.1396		1.0847	
$\int_o^\infty G'(1-G')dY$	0.5470		0.5014		0.4591		0.4382	
H_y	2.518		2.489		2.482		2.475	

TABLE 3/

TABLE 3

$F_o = +0.4$

β ->	-0.371		-0.350		-0.300		-0.200	
Y	z/θ_y	v/V_o	z/θ_y	v/V_o	z/θ_y	v/V_o	z/θ_y	v/V_o
0	0	0	0	0	0	0	0	0
0.5	1.025	0.2784	1.119	0.3009	1.195	0.3187	1.260	0.3338
1.0	2.050	0.5051	2.239	0.5439	2.389	0.5733	2.519	0.5981
1.5	3.076	0.6851	3.359	0.7303	3.584	0.7616	3.779	0.7876
2.0	4.101	0.8195	4.478	0.8595	4.779	0.8857	5.039	0.9045
2.5	5.126	0.9099	5.598	0.9381	5.974	0.9542	6.299	0.9652
3.0	6.151	0.9621	6.717	0.9774	7.168	0.9852	7.559	0.9896
3.5	7.176	0.9870	7.837	0.9933	8.363	0.9957	8.818	0.9978
4.0	8.202	0.9964	3.956	0.9980	9.558	0.9993	10.078	0.9993
4.5	9.227	0.9993	10.076	0.9993	10.753	1.0	11.338	1.0
5.0	10.252	0.9999	11.196	1.0				
5.5	11.277	1.0						
$G''(0)$	0.6144		0.6658		0.7052		0.7402	
$\int_0^\infty (1-G')dY$	1.1658		1.0658		0.9985		0.9466	
$\int_0^\infty G'(1-G')dY$	0.4877		0.4466		0.4185		0.3969	
H_y	2.390		2.386		2.386		2.385	

TABLE 4/

TABLE 4

$F_o = +0.6$

β ->	-0.474		-0.450		-0.400		-0.350	
Y	z/θ_y	v/V_o	z/θ_y	v/V_o	z/θ_y	v/V_o	z/θ_y	v/V_o
0	0	0	0	0	0	0	0	0
0.5	1.152	0.3356	1.259	0.3588	1.317	0.3715	1.353	0.3793
1.0	2.304	0.5826	2.518	0.6195	2.634	0.6390	2.707	0.6508
1.5	3.455	0.7590	3.777	0.7979	3.950	0.8172	4.061	0.8284
2.0	4.607	0.8764	5.036	0.9073	5.267	0.9212	5.414	0.9289
2.5	5.759	0.9456	6.296	0.9644	6.584	0.9719	6.768	0.9758
3.0	6.911	0.9800	7.555	0.9889	7.901	0.9919	8.121	0.9934
3.5	8.063	0.9940	8.814	0.9972	9.218	0.9981	9.475	0.9986
4.0	9.214	0.9985	10.073	0.9994	10.535	0.9996	10.828	0.9998
4.5	10.366	0.9997	11.332	0.9999	11.851	0.9999	12.182	1.0
5.0	11.518	0.9999	12.591	1.0	13.168	1.0		
5.5	12.670	1.0						
G"(0)	0.7771		0.8317		0.8617		0.8801	
$\int_o^\infty (1-G')dY$	0.9982		0.9160		0.8769		0.8542	
$\int_o^\infty G'(1-G')dY$	0.4341		0.3971		0.3797		0.3694	
H_y	2.299		2.307		2.309		2.312	

TABLE 5/

TABLE 5

$F_o = +0.8$

β ->	-0.592		-0.570		-0.550		-0.500	
Y	z/θ_y	v/V_o	z/θ_y	v/V_o	z/θ_y	v/V_o	z/θ_y	v/V_o
0	0	0	0	0	0	0	0	0
0.5	1.290	0.3905	1.378	0.4080	1.406	0.4136	1.460	0.4242
1.0	2.579	0.6503	2.756	0.6763	2.812	0.6843	2.920	0.6995
1.5	3.869	0.8173	4.133	0.8423	4.218	0.8497	4.381	0.8633
2.0	5.159	0.9162	5.511	0.9341	5.624	0.9391	5.841	0.9477
2.5	6.448	0.9674	6.889	0.9771	7.030	0.9796	7.301	0.9837
3.0	7.738	0.9896	8.267	0.9935	8.436	0.9945	8.762	0.9960
3.5	9.028	0.9973	9.644	0.9985	9.842	0.9989	10.222	0.9993
4.0	10.317	0.9994	11.022	0.9997	11.249	0.9998	11.682	1.0
4.5	11.607	0.9999	12.4	1.0	12.655	1.0		
5.0	12.896	1.0						
5.5								
G"(0)	0.9480		0.9912		1.0050		1.0312	
$\int_0^\infty (1-G')dY$	0.8663		0.8146		0.7994		0.7717	
$\int_0^\infty G'(1-G')dY$	0.3877		0.3629		0.3556		0.3424	
H_y	2.234		2.245		2.248		2.254	

TABLE 6/

TABLE 6

$F_o = +1.0$

$\beta \rightarrow$	-0.721		-0.70		-0.65		-0.60	
Y	z/θ_y	v/V_o	z/θ_y	v/V_o	z/θ_y	v/V_o	z/θ_y	v/V_o
0	0	0	0	0	0	0	0	0
0.5	1.433	0.4425	1.513	0.4563	1.577	0.4677	1.621	0.4752
1.0	2.866	0.7087	3.026	0.7278	3.153	0.7430	3.241	0.7529
1.5	4.299	0.8624	4.539	0.8793	4.730	0.8920	4.862	0.8999
2.0	5.732	0.9436	6.051	0.9544	6.307	0.9620	6.483	0.9665
2.5	7.165	0.9805	7.564	0.9858	7.884	0.9892	8.104	0.9912
3.0	8.598	0.9944	9.077	0.9965	9.461	0.9976	9.724	0.9983
3.5	10.031	0.9985	10.590	0.9993	11.037	0.9996	11.345	1.0
4.0	11.465	0.9995	12.103	0.9999	12.614	1.0		
4.5	12.898	0.9997	13.616	1.0				
5.0	14.331	0.9998						
5.5	15.764	1.0						

$G''(0)$	1.1256	1.1613	1.1907	1.2102
$\int_0^\infty (1-G')dY$	0.7619	0.7262	0.7002	0.6829
$\int_0^\infty G'(1-G')dY$	0.3489	0.3305	0.3171	0.3085
H_y	2.184	2.197	2.208	2.214

TABLE 7/

TABLE 7

$\beta = -1$

F_o ->	1.414		1.421		1.437		1.500		1.554	
Y	z/θ_y	v/V_o	z/θ_y	v/V_o	z/θ_y	v/V_o	z/θ_y	v/V_o	z/θ_y	v/V_o
0	0	0	0	0	0	0	0	0	0	0
0.25	0.880	0.3169	0.903	0.3218	0.925	0.3270	0.980	0.3420	1.015	0.3527
0.50	1.760	0.5396	1.806	0.5469	1.850	0.5548	1.959	0.5761	2.030	0.5907
0.75	2.640	0.6947	2.709	0.7035	2.776	0.7120	2.939	0.7342	3.045	0.7485
1.0	3.520	0.8023	3.613	0.8109	3.701	0.8190	3.918	0.8388	4.060	0.8510
1.25	4.400	0.8757	4.516	0.8832	4.626	0.8901	4.898	0.9060	5.075	0.9153
1.50	5.280	0.9245	5.419	0.9305	5.551	0.9359	5.878	0.9476	6.090	0.9540
1.75	6.160	0.9559	6.322	0.9604	6.477	0.9642	6.857	0.9721	7.105	0.9763
2.0	7.040	0.9754	7.225	0.9784	7.402	0.9810	7.837	0.9859	8.120	0.9884
2.25	7.920	0.9869	8.129	0.9889	8.327	0.9904	8.817	0.9933	9.135	0.9946
2.50	8.800	0.9934	9.032	0.9945	9.252	0.9954	9.796	0.9970	10.150	0.9977
2.75	9.680	0.9968	9.935	0.9975	10.178	0.9979	10.776	0.9987	11.165	0.9990
3.0	10.560	0.9986	10.838	0.9989	11.103	0.9991	11.755	0.9995	12.180	0.9996
3.25	11.440	0.9994	11.741	0.9995	12.028	0.9996	12.735	0.9998	13.195	0.9999
3.50	12.320	0.9997	12.644	0.9998	12.953	0.9999	13.715	0.9999	14.210	1.0
3.75	13.200	0.9999	13.548	0.9999	13.879	1.0	14.694	1.0		
4.0	14.079	1.0	14.451	1.0						

G"(0)	1.5049	1.5294	1.5574	1.6413	1.7030
$\int_0^\infty (1-G')dY$	0.6023	0.5884	0.5753	0.5437	0.5243
$\int_0^\infty G'(1-G')dY$	0.2841	0.2768	0.2702	0.2552	0.2463
H_y	2.120	2.126	1.129	2.130	2.129

TABLE 8

TABLE 8

$\beta = -\infty$ or $m = -1$

z/θ_y	v/V_o
0	0
0.2	0.0952
0.4	0.1813
0.6	0.2592
0.8	0.3207
1.0	0.3935
1.4	0.5034
1.8	0.5934
2.0	0.6321
2.4	0.6988
2.8	0.7534
3.2	0.7981
3.6	0.8347
4.0	0.8647
4.4	0.8892
4.8	0.9093
5.2	0.9257
5.6	0.9392
6.0	0.9502
8.0	0.9817
10.0	0.9933
12.0	0.9959
14.0	0.9991
∞	1.0

TABLE 9/

TABLE 9

F_o->	0		0.5		1.095			1.9265			2.664	
η	z/θ_y	v/V_o	z/θ_y	v/V_o	η	z/θ_y	v/V_o	η	z/θ_y	v/V_o	η	z/θ_y	v/V_o
0	0	0	0	0	0	0	0	0	0	0	0	0	0
0.1	0.2477	0.0570	0.3040	0.090	0.049	0.1872	0.0670	0.022	0.1121	0.0462	0.026	0.1650	0.0711
0.2	0.4954	0.1141	0.6081	0.1755	0.149	0.5693	0.1931	0.122	0.6218	0.2331	0.126	0.7595	0.3031
0.3	0.7431	0.1709	0.9121	0.2566	0.249	0.9515	0.3059	0.222	1.131	0.3869	0.266	1.434	0.4804
0.4	0.9908	0.2275	1.216	0.3333	0.349	1.334	0.4065	0.322	1.641	0.5131	0.326	2.038	0.6154
0.5	1.238	0.2836	1.520	0.4055	0.449	1.716	0.4957	0.422	2.151	0.6161	0.426	2.703	0.7175
0.6	1.486	0.3389	1.824	0.4731	0.549	2.098	0.5744	0.522	2.660	0.6996	0.526	3.337	0.7942
0.7	1.734	0.3932	2.128	0.5360	0.649	2.480	0.6434	0.622	3.170	0.7668	0.626	3.972	0.8513
0.8	1.982	0.4462	2.432	0.5941	0.749	2.862	0.7034	0.722	3.680	0.8205	0.726	4.607	0.8936
0.9	2.229	0.4976	2.736	0.6474	0.849	3.244	0.7552	0.822	4.189	0.8630	0.826	5.241	0.9245
1.0	2.477	0.5470	3.040	0.6960	0.949	3.626	0.7996	0.922	4.699	0.8963	0.926	5.875	0.9469
1.1	2.725	0.5942	3.344	0.7398	1.049	4.008	0.8373	1.022	5.209	0.9223	1.026	6.150	0.9630
1.2	2.972	0.6389	3.648	0.7791	1.149	4.390	0.8690	1.122	5.719	0.9422	1.126	7.145	0.9745
1.3	3.220	0.6810	3.953	0.8139	1.249	4.773	0.8955	1.222	6.228	0.9575	1.226	7.779	0.9827
1.4	3.468	0.7201	4.257	0.8445	1.349	5.155	0.9173	1.322	6.738	0.9690	1.326	8.414	0.9883
1.5	3.716	0.7563	4.561	0.8712	1.449	5.537	0.9351	1.422	7.248	0.9776	1.426	9.048	0.9922
1.6	3.963	0.7894	4.865	0.8942	1.549	5.919	0.9496	1.522	7.757	0.9840	1.526	9.683	0.9948
1.7	4.211	0.8194	5.169	0.9139	1.649	6.301	0.9612	1.622	8.267	0.9886	1.626	10.317	0.9966
1.8	4.459	0.8463	5.473	0.9305	1.749	6.683	0.9704	1.722	8.777	0.9920	1.726	10.952	0.9979
1.9	4.706	0.8703	5.777	0.9445	1.849	7.065	0.9777	1.822	9.286	0.9945	1.826	11.586	0.9989
2.0	4.954	0.8915	6.081	0.9561	1.949	7.447	0.9833	1.922	9.796	0.9962	1.926	12.221	0.9992
2.1	5.202	0.9099	6.385	0.9656	2.049	7.830	0.9876	2.022	10.306	0.9975	2.026	12.855	0.9995
2.2	5.450	0.9258	6.689	0.9733	2.149	8.212	0.9910	2.122	10.815	0.9983	2.126	13.490	0.9997

TABLE 9 (contd.)/

TABLE 9 (Contd.)

F_o->	0		0.5		1.095			1.9265			2.664		
η	z/θ_y	v/V_o	z/θ_y	v/V_o	η	z/θ_y	v/V_o	η	z/θ_y	v/V_o	η	z/θ_y	v/V_o
2.3	5.697	0.9395	6.993	0.9796	2.249	8.594	0.9935	2.222	11.325	0.9989	2.226	14.124	0.9999
2.4	5.945	0.9511	7.297	0.9846	2.349	8.976	0.9953	2.322	11.835	0.9993	2.326	14.759	1.0
2.5	6.193	0.9608	7.601	0.9885	2.449	9.358	0.9967	2.422	12.344	0.9996	2.426		
2.6	6.440	0.9688	7.905	0.9916	2.549	9.740	0.9978	2.522	12.854	0.9998	2.526		
2.7	6.688	0.9755	8.209	0.9940	2.649	10.122	0.9985	2.622	13.364	0.9999			
2.8	6.936	0.9809	8.513	0.9958	2.749	10.504	0.9990	2.722	13.874	1.0			
2.9	7.183	0.9852	8.817	0.9972	2.849	10.886	0.9994						
3.0	7.431	0.9887	9.121	0.9982	2.949	11.269	0.9997						
3.1	7.679	0.9914	9.425	0.9990	3.049	11.651	0.9999						
3.2	7.927	0.9936	9.729	0.9996	3.149	12.033	1.0						
3.3	8.174	0.9952	10.033	1.00									
3.4	8.422	0.9965											
3.5	8.670	0.9975											
3.6	8.917	0.9982											
3.7	9.165	0.9988											
3.8	9.413	0.9992											
3.9	9.661	0.9994											
4.0	9.908	0.9997											
4.1	10.156	0.9998											
4.2	10.404	0.9999											
4.3	10.651	1.0											

TABLE 9 (contd.)/

TABLE 9 (Contd.)

F_o - >	0	0.5	1.095	1.9265	2.664
G"(0)	0.5705	0.9226	1.4052	2.1441	2.8329
$\int_0^\infty (1-G')dY$	1.0256	0.77300	0.5797	0.4162	0.3279
$\int_0^\infty G'(1-G')dY$	0.4037	0.3289	0.2617	0.1962	0.1576
H_y	2.5405	2.3502	2.2151	2.1213	2.0806

BW

Addendum

8. The Application of These Solutions to a Particular Class of Heat-transfer Problem

Neglecting the heat generated by dissipation and assuming a Prandtl number of unity, the temperature distribution in the laminar boundary layer on a porous cylinder, uniformly heated to a fixed temperature T_1 and held in a stream at temperature T_0, is given in the present notation by

$$u\frac{\partial T}{\partial x} + w\frac{\partial T}{\partial z} = \frac{\partial^2 T}{\partial z^2} \qquad \ldots(57)$$

The boundary conditions are

$$T = T_1 \quad \text{at} \quad z = 0 ,$$

and $\qquad \ldots(58)$

$$T = T_0 \quad \text{at} \quad z = \alpha ,$$

Then, putting $\theta(\eta) = \dfrac{T_1 - T}{T_1 - T_0}$, equation (57) reduces to

$$\theta'' + \tfrac{1}{2}(m + 1) f\theta' = 0 , \qquad \ldots(59)$$

with the boundary conditions

$$\theta = 0 \quad \text{at} \quad \eta = 0 ,$$

$$\theta = 1 \quad \text{at} \quad \eta = \alpha ,$$

and when continuous suction is applied on the cylinder $f(0)$ is a non-zero positive quantity.

Equation (59) is identical with equation (12), with the same boundary conditions. Hence solutions for $g'(\eta)$ (the spanwise velocity) in equation (12) will provide solutions for $\theta(\eta)$ in equation (59), for those cases of two-dimensional laminar boundary-layer flow which have been used for the calculations of spanwise velocity.

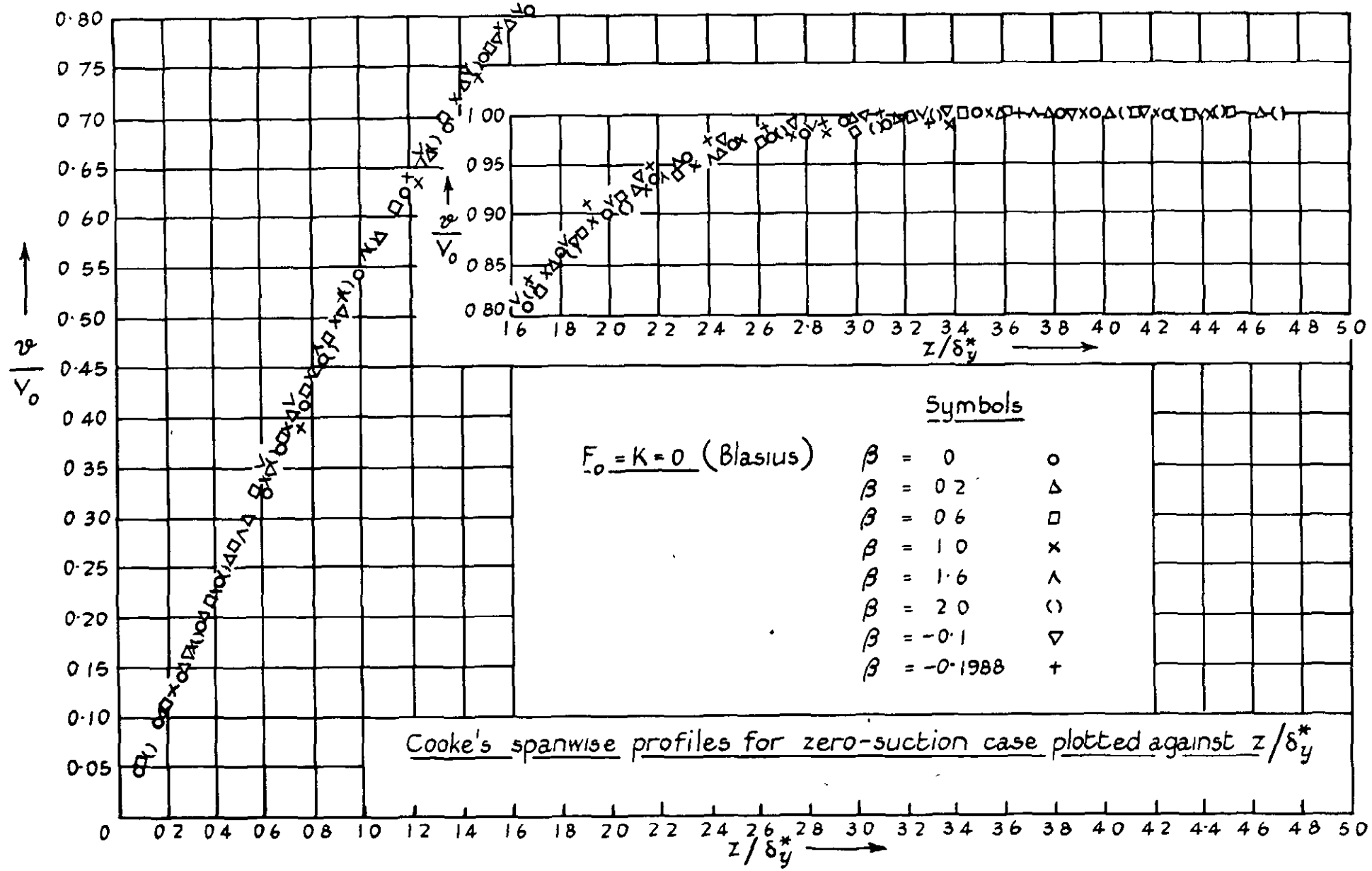
w/V_0
z/δ_y^*
$F_0 = K = 0$ (Blasius)
Symbols
$\beta = 0$ o
$\beta = 0.2$ Δ
$\beta = 0.6$ □
$\beta = 1.0$ ×
$\beta = 1.6$ ^
$\beta = 2.0$ ( )
$\beta = -0.1$ ▽
$\beta = -0.1988$ +
Cooke's spanwise profiles for zero-suction case plotted against z/δ_y^*

FIG 1.

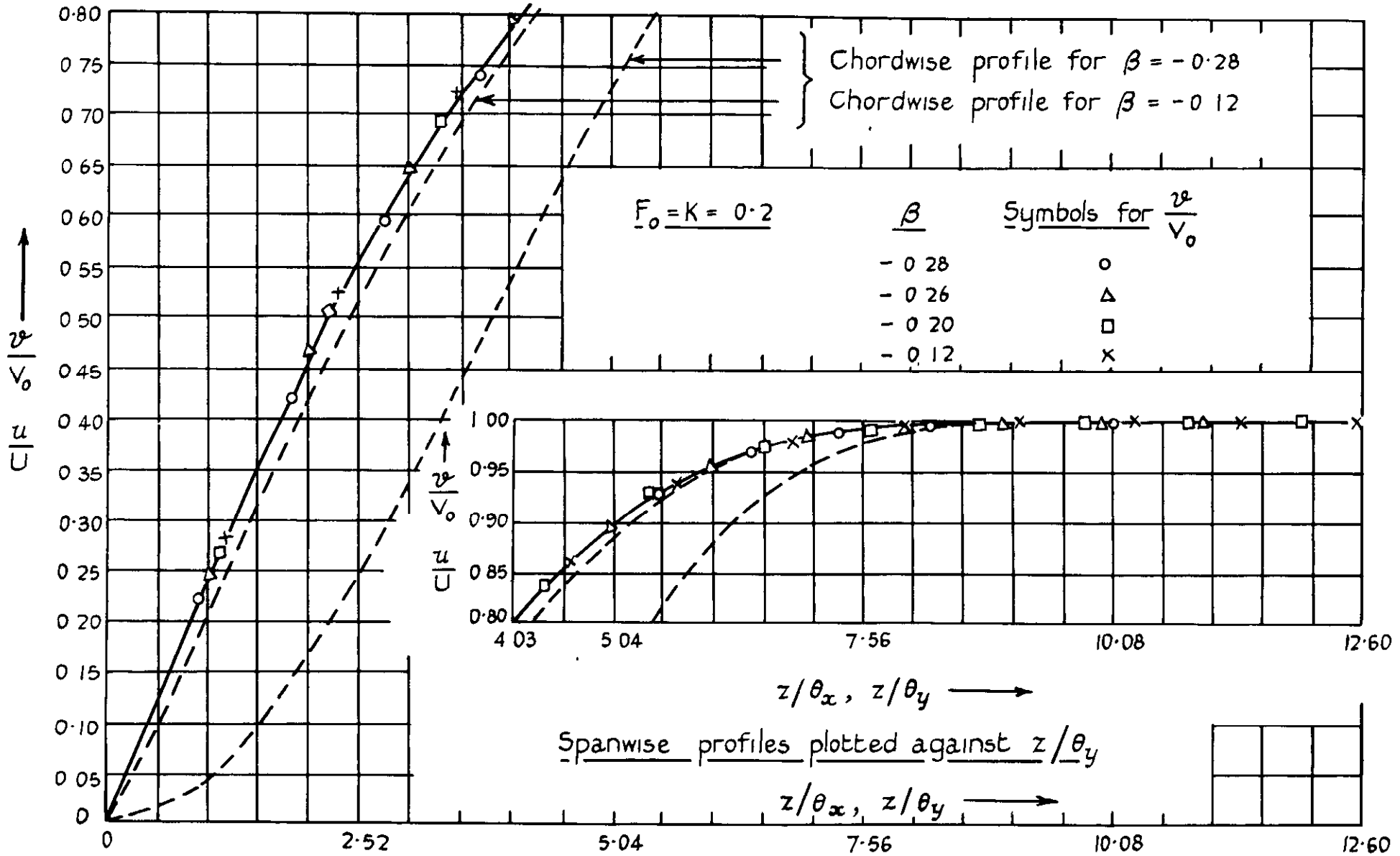
Chordwise profile for β = - 0·28
Chordwise profile for β = - 0 12
F₀ = K = 0·2
β
Symbols for v/V₀
- 0 28
- 0 26
- 0 20
- 0 12
v/V₀
u/U
z/θx , z/θy
Spanwise profiles plotted against z/θy
0·80
0 75
0 70
0 65
0 60
0 55
0 50
0 45
0 40
0 35
0·30
0 25
0 20
0 15
0·10
0 05
0
2·52
5·04
7·56
10·08
12·60
1 00
0·95
0·90
0 85
0·80
4 03
5 04

FIG. 2.

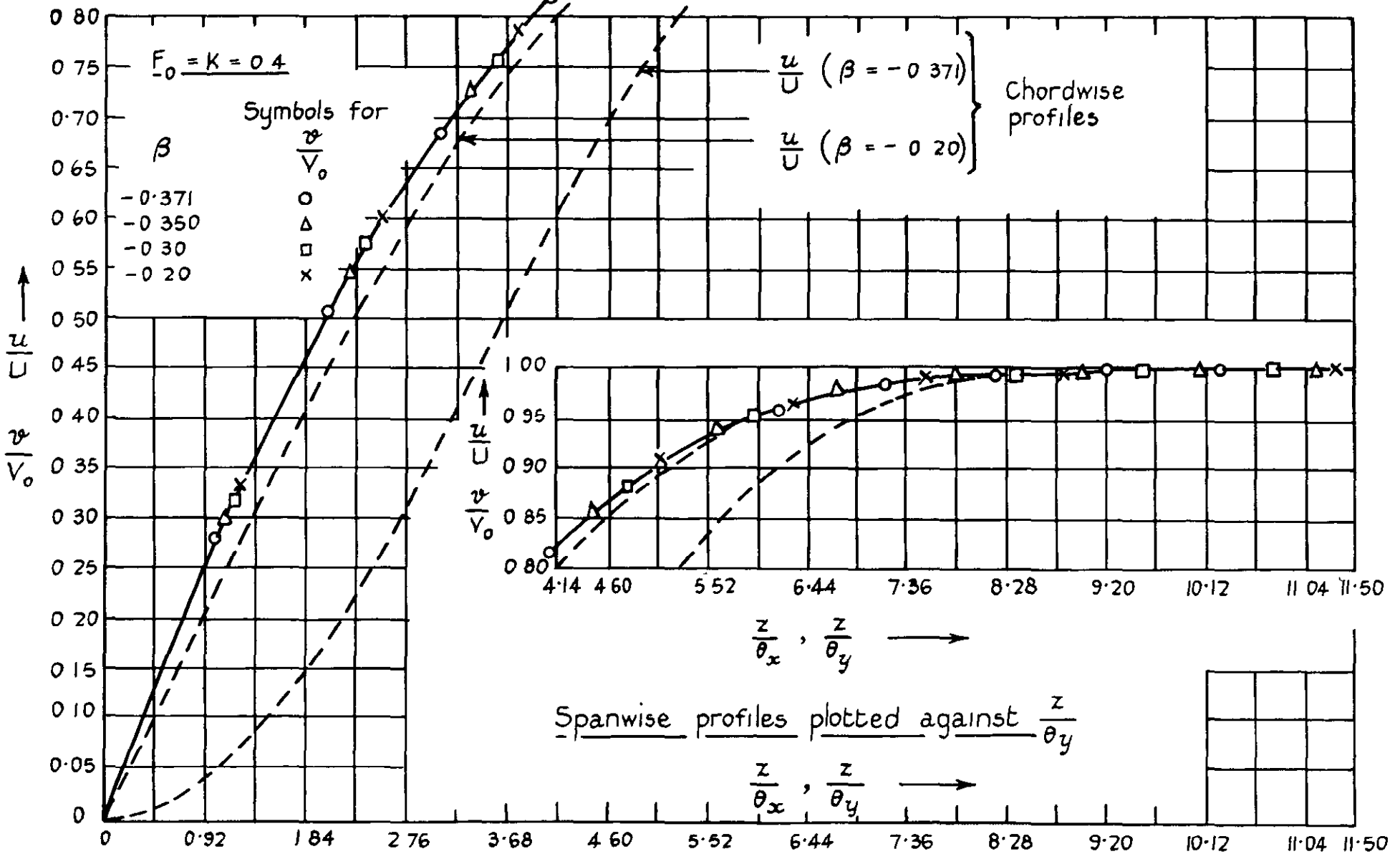
$F_0 = K = 0.4$
Symbols for
β
$\frac{v}{V_0}$
-0·371 ○
-0 350 △
-0 30 □
-0 20 ×
$\frac{u}{U}$ ($\beta = -0\ 371$)
$\frac{u}{U}$ ($\beta = -0\ 20$)
Chordwise profiles
$\frac{u}{U}$
$\frac{v}{V_0}$
0 80 0 75 0·70 0 65 0 60 0 55 0 50 0 45 0 40 0 35 0 30 0 25 0 20 0 15 0 10 0·05 0
0 0·92 1 84 2 76 3·68 4 60 5·52 6·44 7·36 8·28 9·20 10·12 11·04 11·50
$\frac{z}{\theta_x}$, $\frac{z}{\theta_y}$ →
1 00 0 95 0 90 0 85 0 80
4·14 4 60 5 52 6·44 7·36 8·28 9·20 10·12 11 04 11·50
$\frac{z}{\theta_x}$, $\frac{z}{\theta_y}$ →
Spanwise profiles plotted against $\frac{z}{\theta_y}$

FIG. 3.

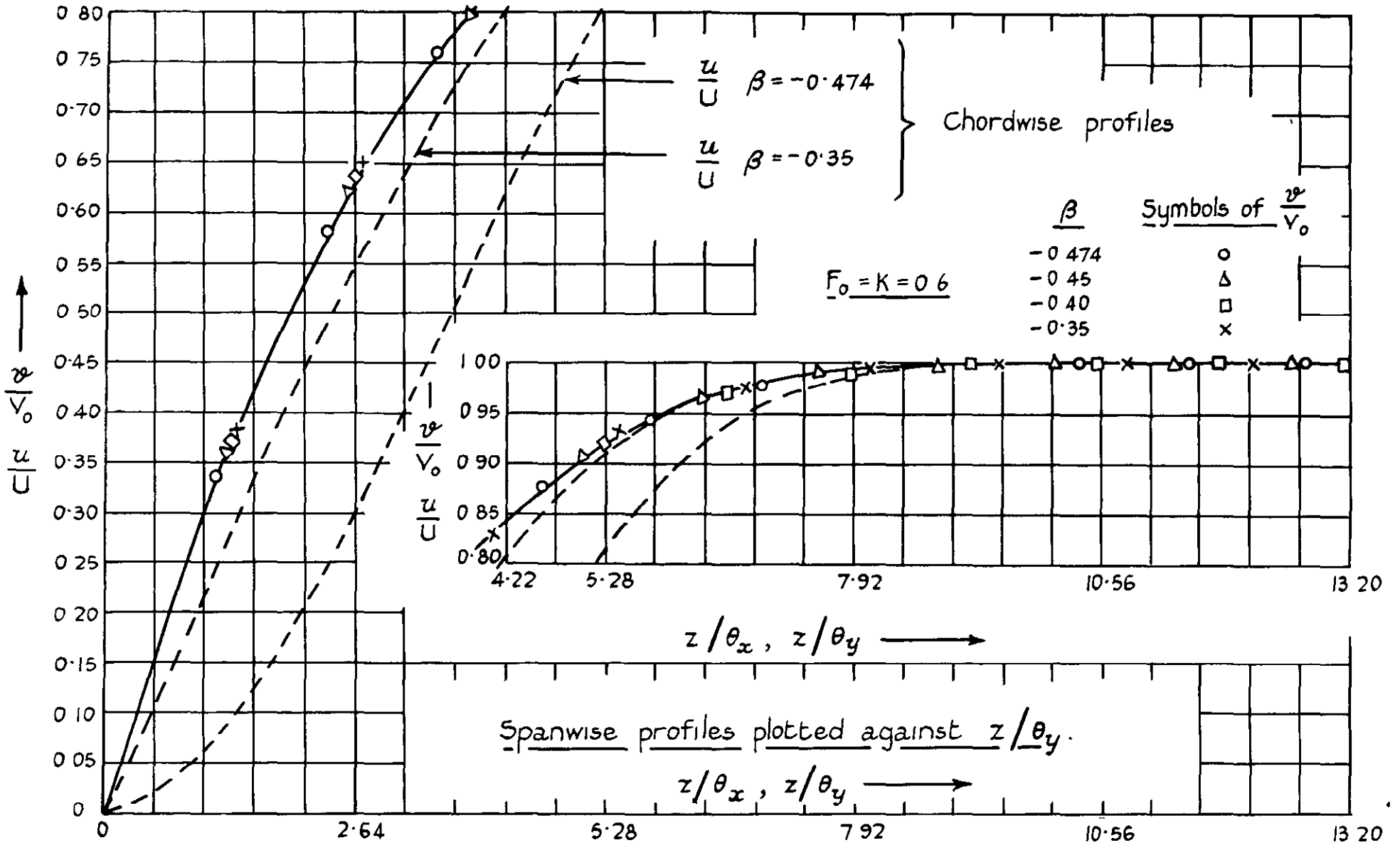
0 80
0 75
0·70
0 65
0·60
0 55
0 50
0·45
0 40
0·35
0·30
0 25
0 20
0·15
0 10
0 05
0
0
2·64
5·28
7 92
10·56
13 20
u/U
v/V₀
u/U β = −0·474
u/U β = −0·35
Chordwise profiles
β
Symbols of v/V₀
−0 474
−0 45
−0 40
−0·35
F₀ = K = 0 6
1 00
0 95
0 90
0 85
0·80
4·22
5·28
7·92
10·56
13 20
z/θx , z/θy
Spanwise profiles plotted against z/θy.
z/θx , z/θy

FIG 4.

FIG 5.

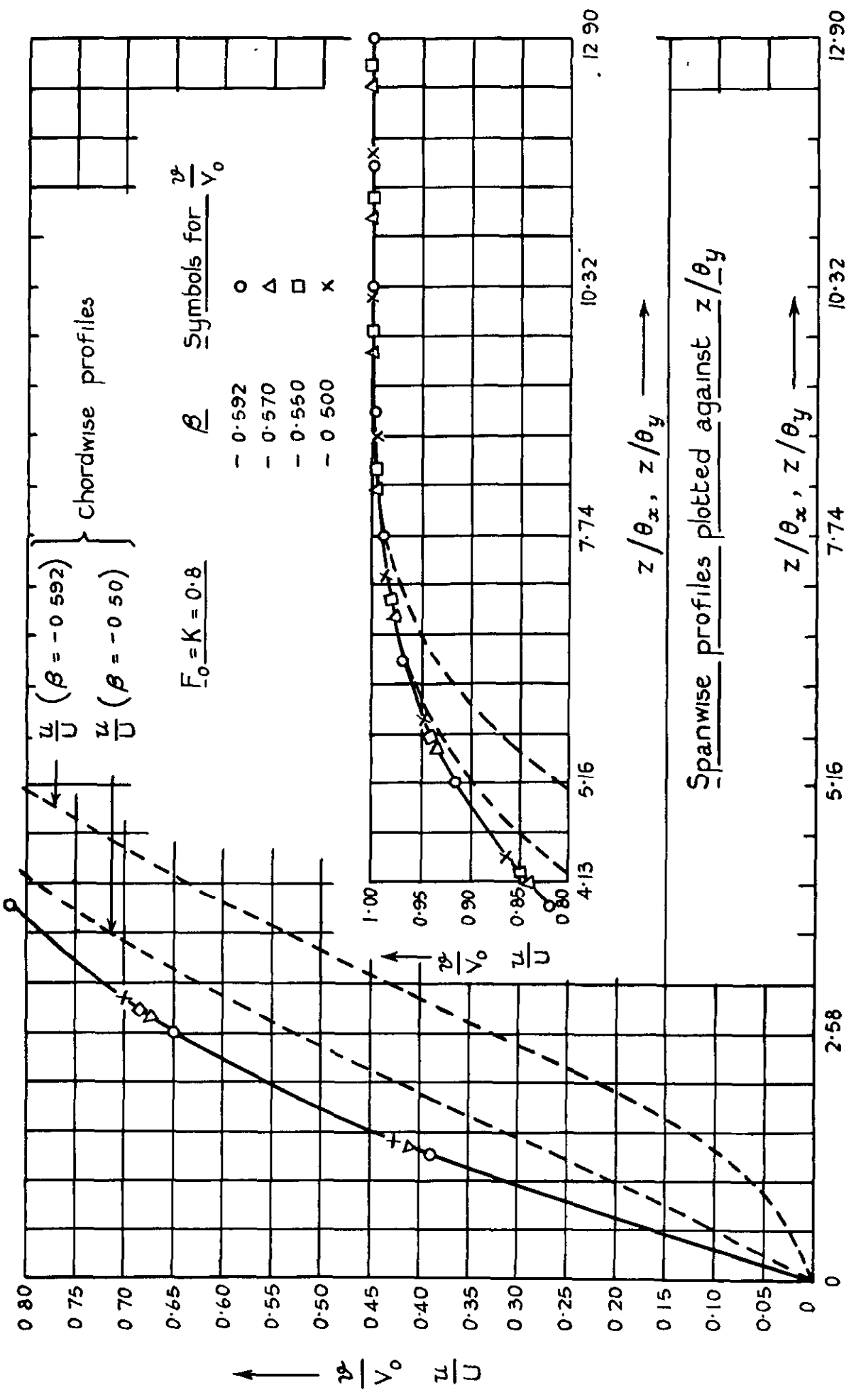
Chordwise profiles
$\frac{u}{U}$ ($\beta = -0.592$)
$\frac{u}{U}$ ($\beta = -0.50$)
$F_0 = K = 0.8$
β Symbols for $\frac{v}{V_0}$
-0.592 o
-0.570 Δ
-0.550 □
-0.500 ×
Spanwise profiles plotted against z/θ_y
z/θ_x, z/θ_y
$\frac{v}{V_0}$ $\frac{u}{U}$
0.80 0.75 0.70 0.65 0.60 0.55 0.50 0.45 0.40 0.35 0.30 0.25 0.20 0.15 0.10 0.05 0
2.58 5.16 7.74 10.32 12.90
1.00 0.95 0.90 0.85 0.80
4.13 5.16 7.74 10.32 12.90

FIG 6.

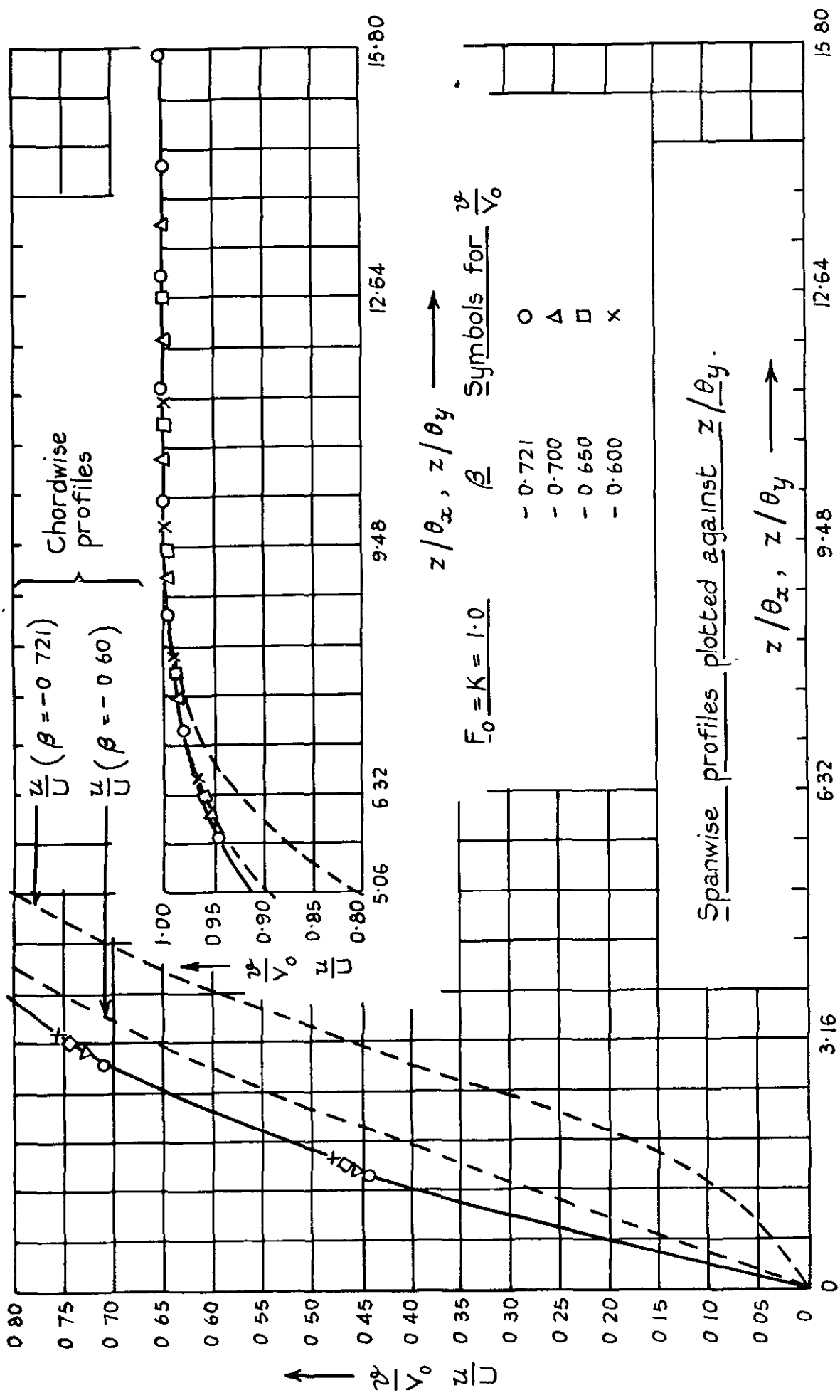
Chordwise profiles
u/U (β = -0 721)
u/U (β = - 0 60)
y/Y₀
u/U
1·00
0·95
0·90
0·85
0·80
5·06
6 32
9·48
12·64
15·80
z/θx , z/θy
F₀ = K = 1·0
β
Symbols for y/Y₀
- 0·721
- 0·700
- 0 650
- 0·600
Spanwise profiles plotted against z/θy.
z/θx , z/θy
0 80
0 75
0 70
0 65
0 60
0 55
0 50
0 45
0 40
0 35
0 30
0 25
0 20
0 15
0 10
0 05
0
3·16
6·32
9·48
12·64
15 80

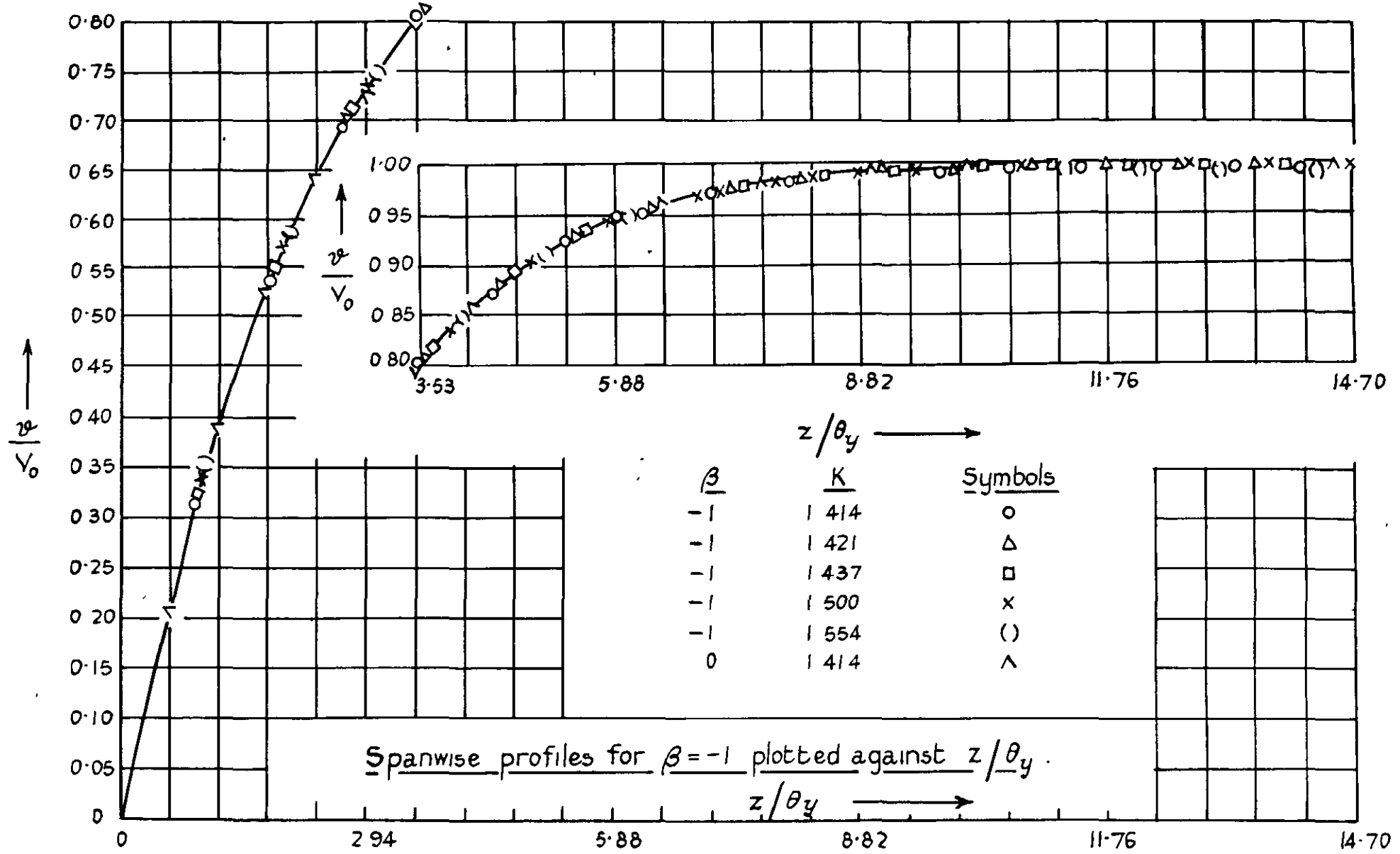
0·80
0·75
0·70
0 65
0·60
0 55
0·50
0 45
0 40
0 35
0 30
0·25
0 20
0·15
0·10
0·05
0
v/V0
1·00
0 95
0 90
0 85
0 80
3·53
5·88
8·82
11·76
14·70
z/θy
β K Symbols
−1 1 414 o
−1 1 421 Δ
−1 1 437 □
−1 1 500 x
−1 1 554 ()
0 1 414 ^
Spanwise profiles for β = −1 plotted against z/θy.
0 2 94 5·88 8·82 11·76 14·70

FIG. 7.

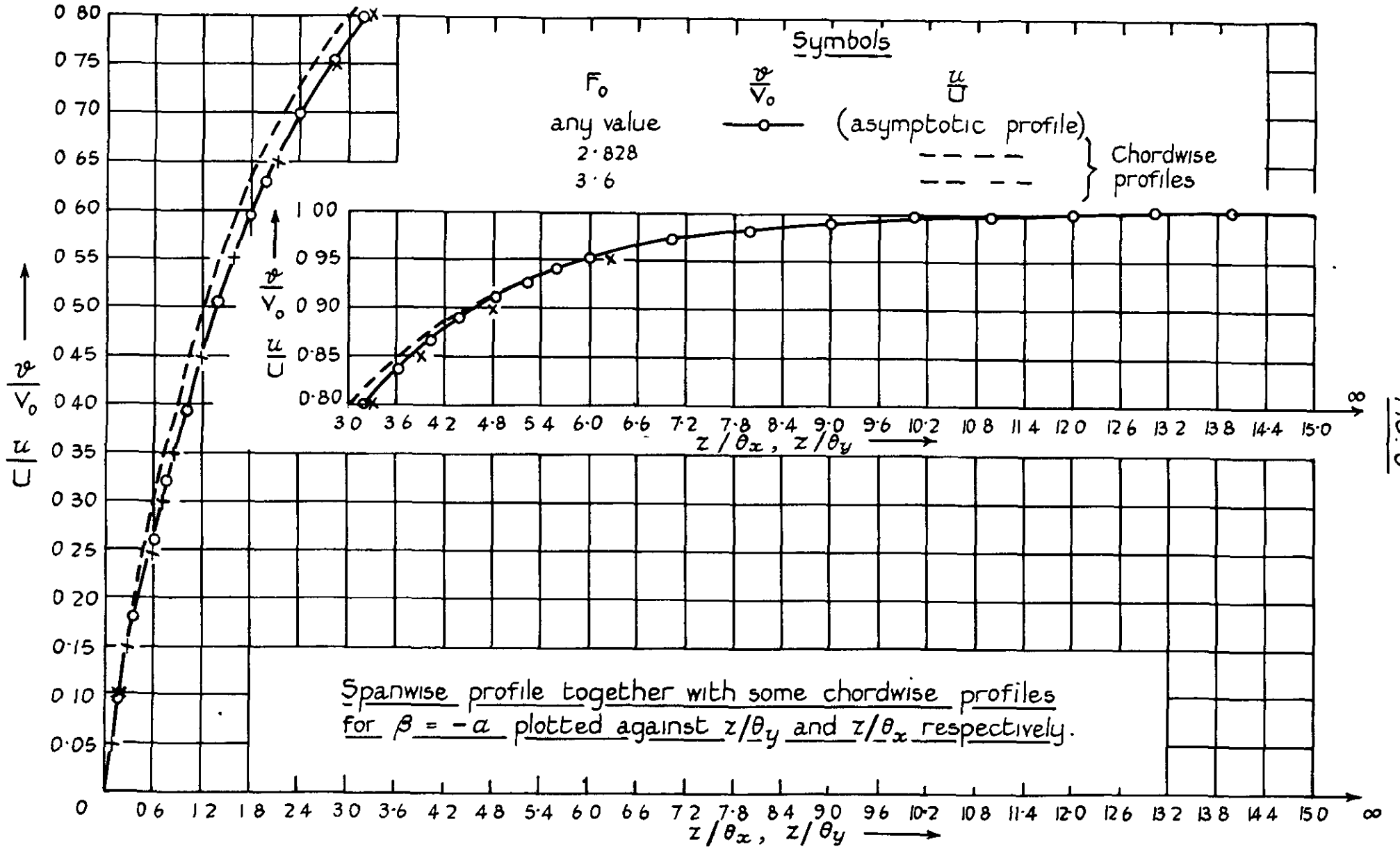
Symbols
F_0
$\frac{v}{V_0}$
$\frac{u}{U}$
any value
2·828
3·6
(asymptotic profile)
Chordwise profiles
$\frac{v}{V_0}$
$\frac{u}{U}$
z/θ_x, z/θ_y
Spanwise profile together with some chordwise profiles for $\beta = -\alpha$ plotted against z/θ_y and z/θ_x respectively.

FIG. 8

FIG 9.

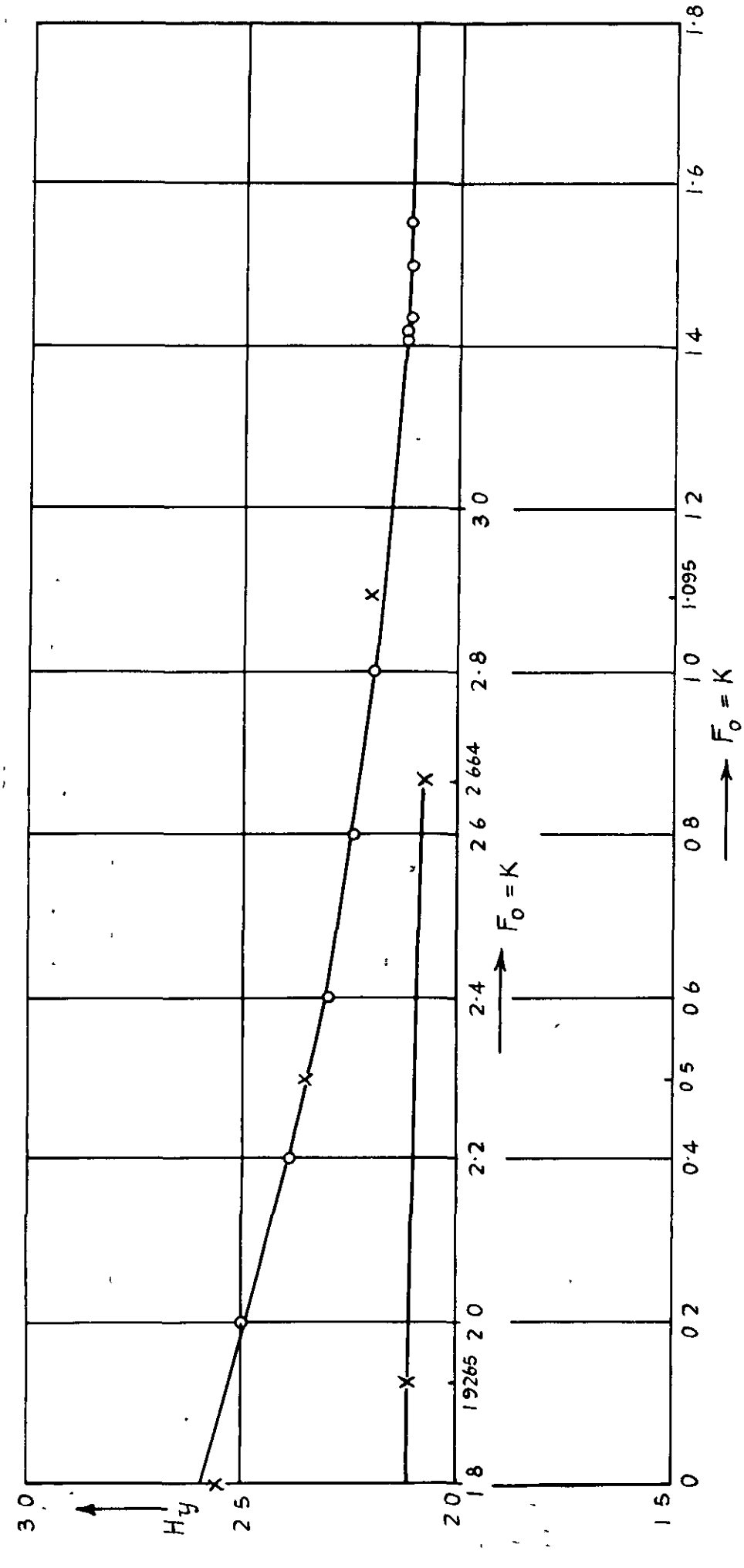

H_y plotted against K for values of β

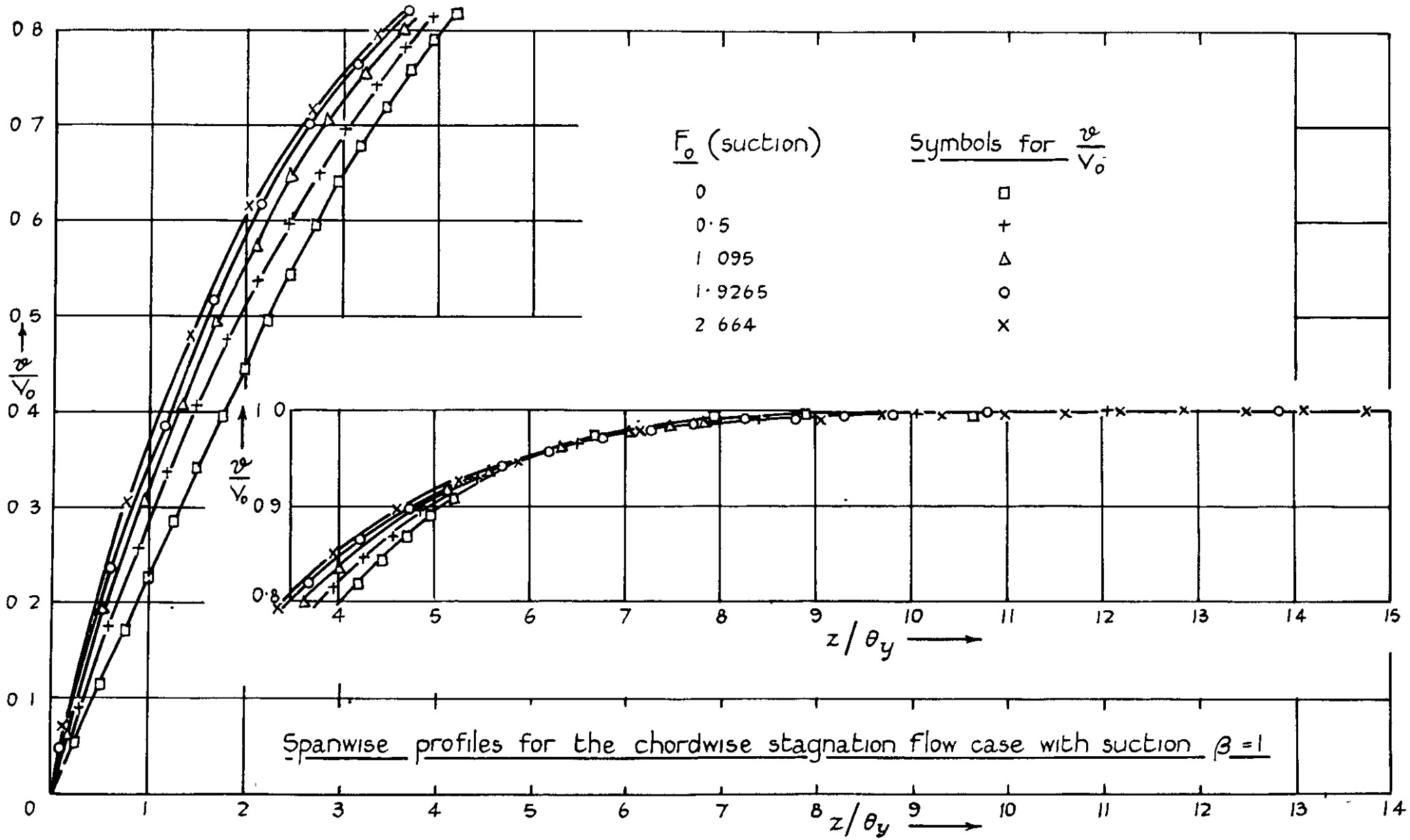
F_o (suction)
Symbols for $\frac{v}{V_o}$
0
0·5
1 095
1·9265
2 664
$\frac{v}{V_o}$
z/θ_y
Spanwise profiles for the chordwise stagnation flow case with suction $\beta = 1$

FIG 10

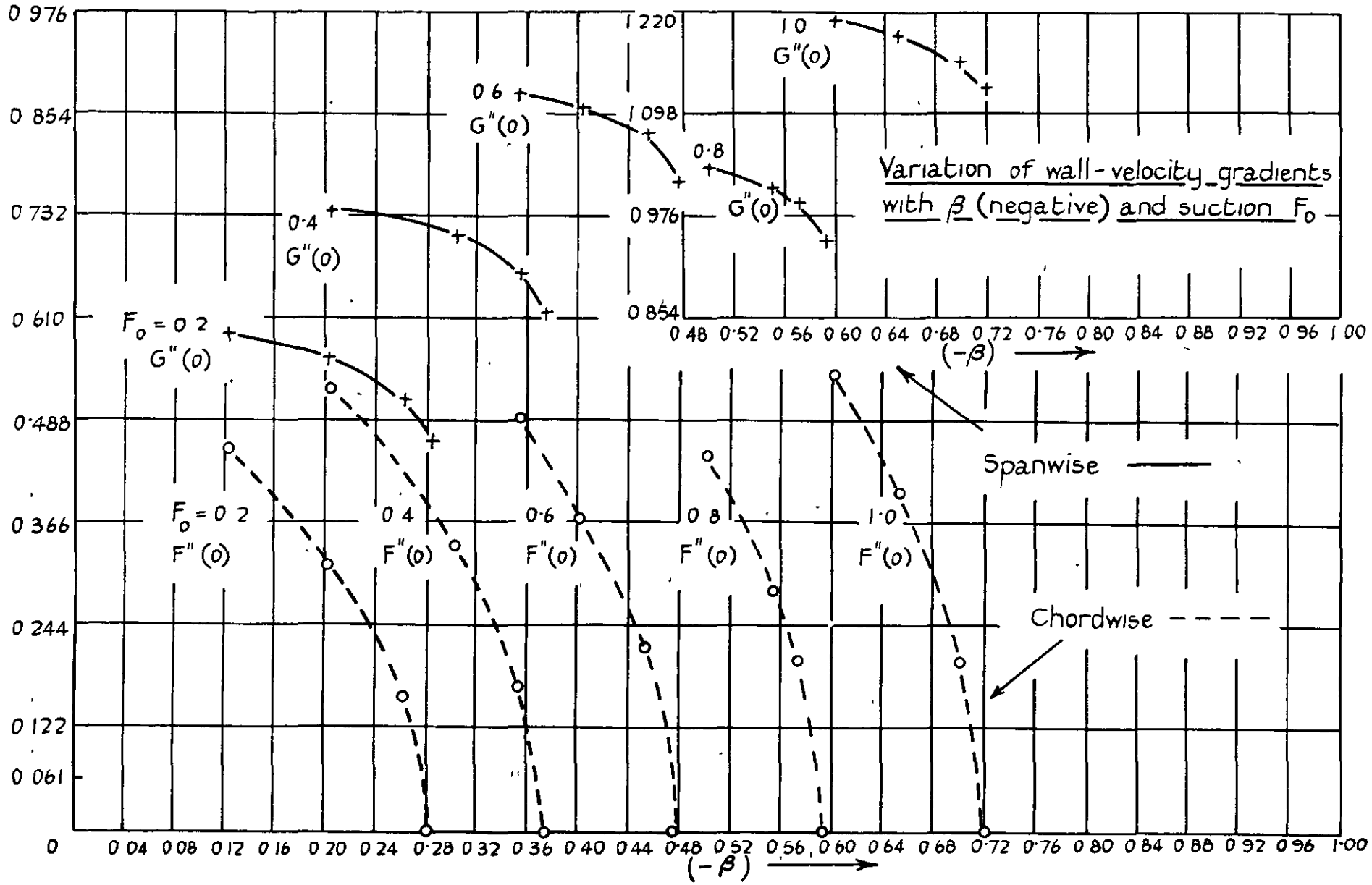
Variation of wall-velocity gradients with β (negative) and suction F0
Spanwise
Chordwise
(−β)
G"(0)
F"(0)
F0 = 0 2
0 4
0·6
0 8
1·0
0·8
0 976
0 854
0 732
0 610
0·488
0 366
0 244
0 122
0 061
0
1 220
1 098
0 48 0·52 0 56 0 60 0 64 0·68 0 72 0·76 0 80 0 84 0 88 0 92 0 96 1 00
0 04 0 08 0 12 0 16 0 20 0 24 0·28 0 32 0 36 0 40 0 44 0·48 0 52 0 56 0 60 0 64 0 68 0·72 0·76 0 80 0 84 0 88 0 92 0 96 1·00

FIG 11.

FIG 12

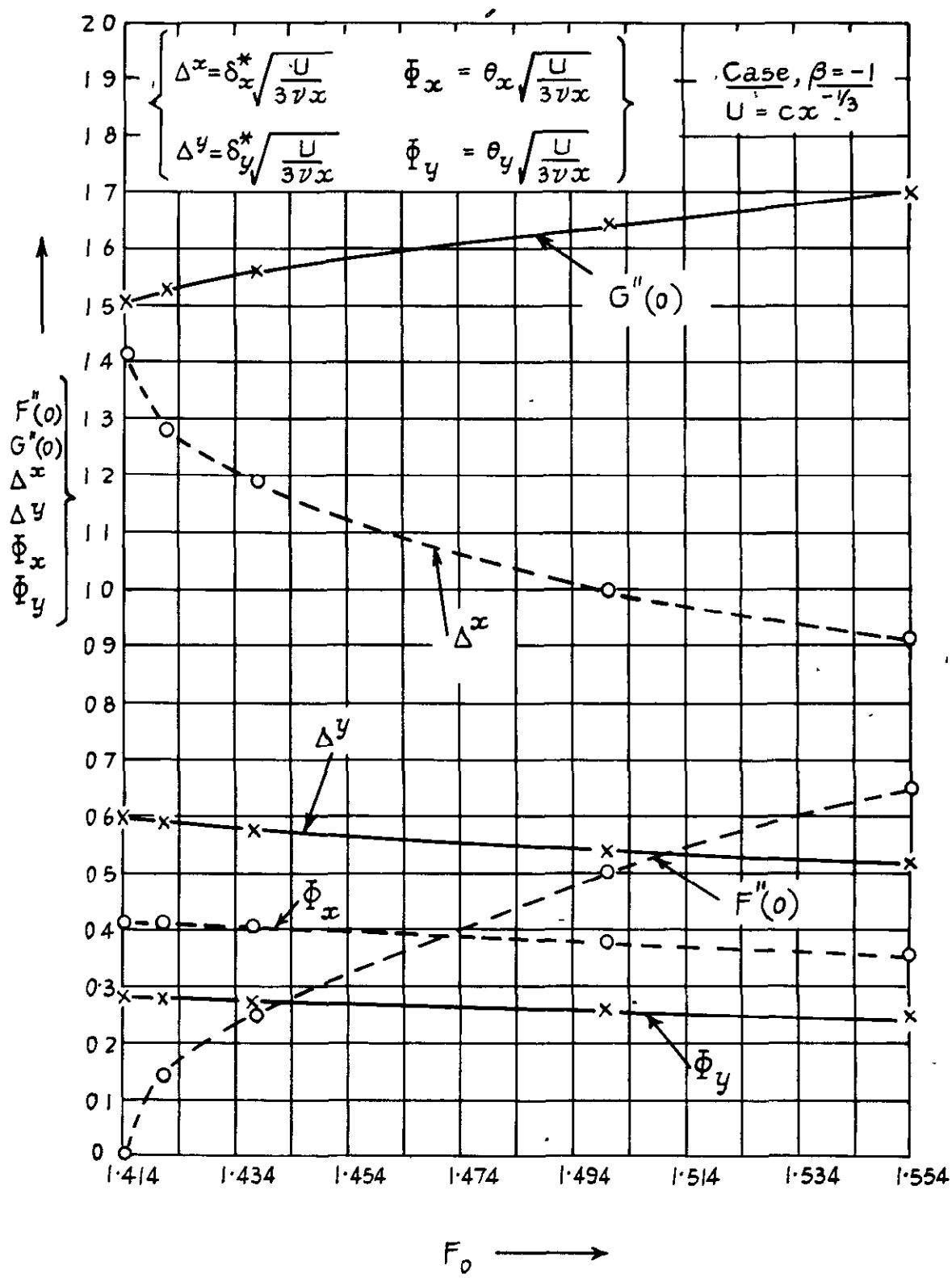

Wall-velocity-gradient, momentum thickness, and displacement thickness plotted against K

FIG 13.

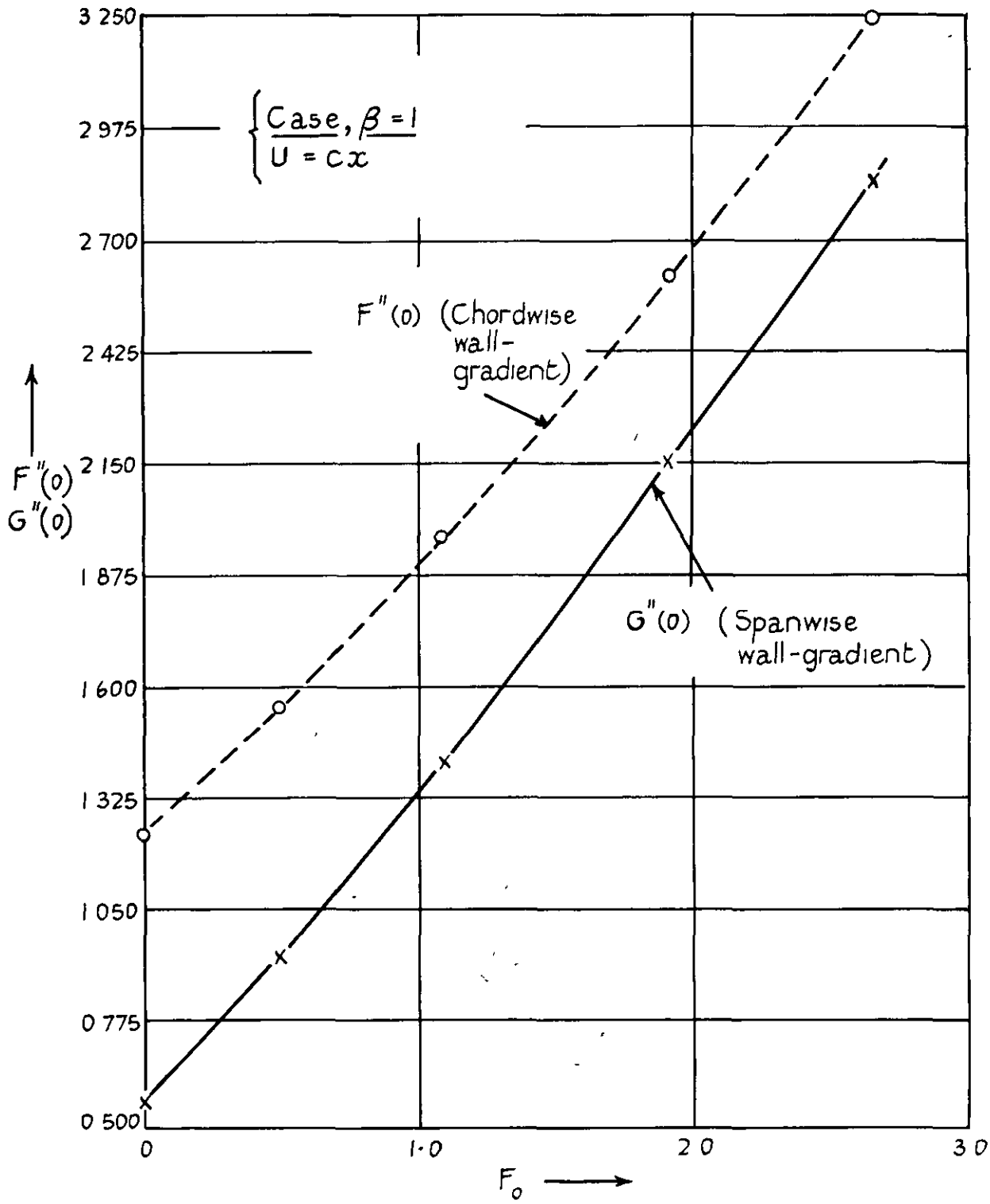

Wall-velocity gradients plotted against K

OT

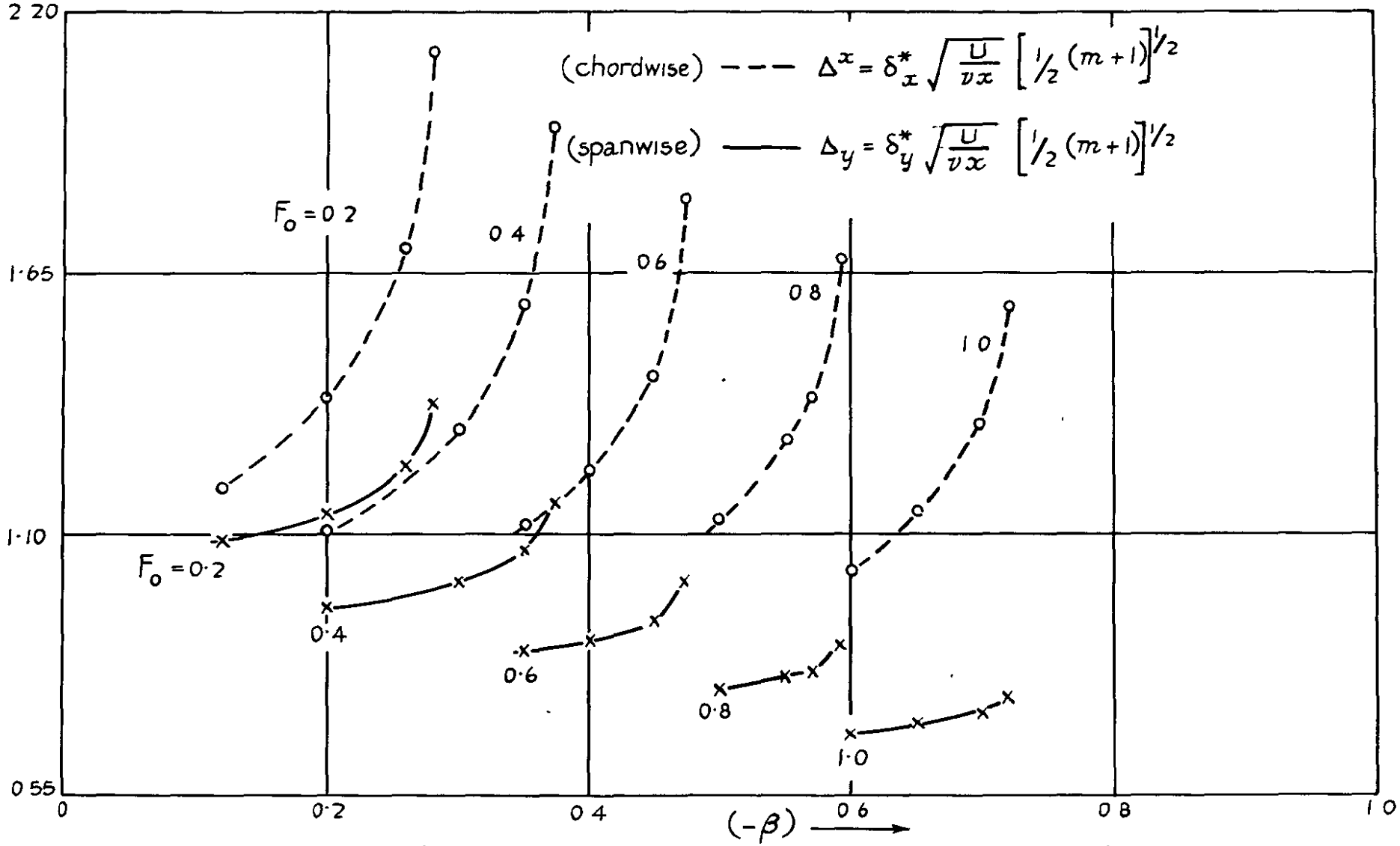

FIG. 14.

Variation of displacement thickness with suction and β(negative)

FIG 15.

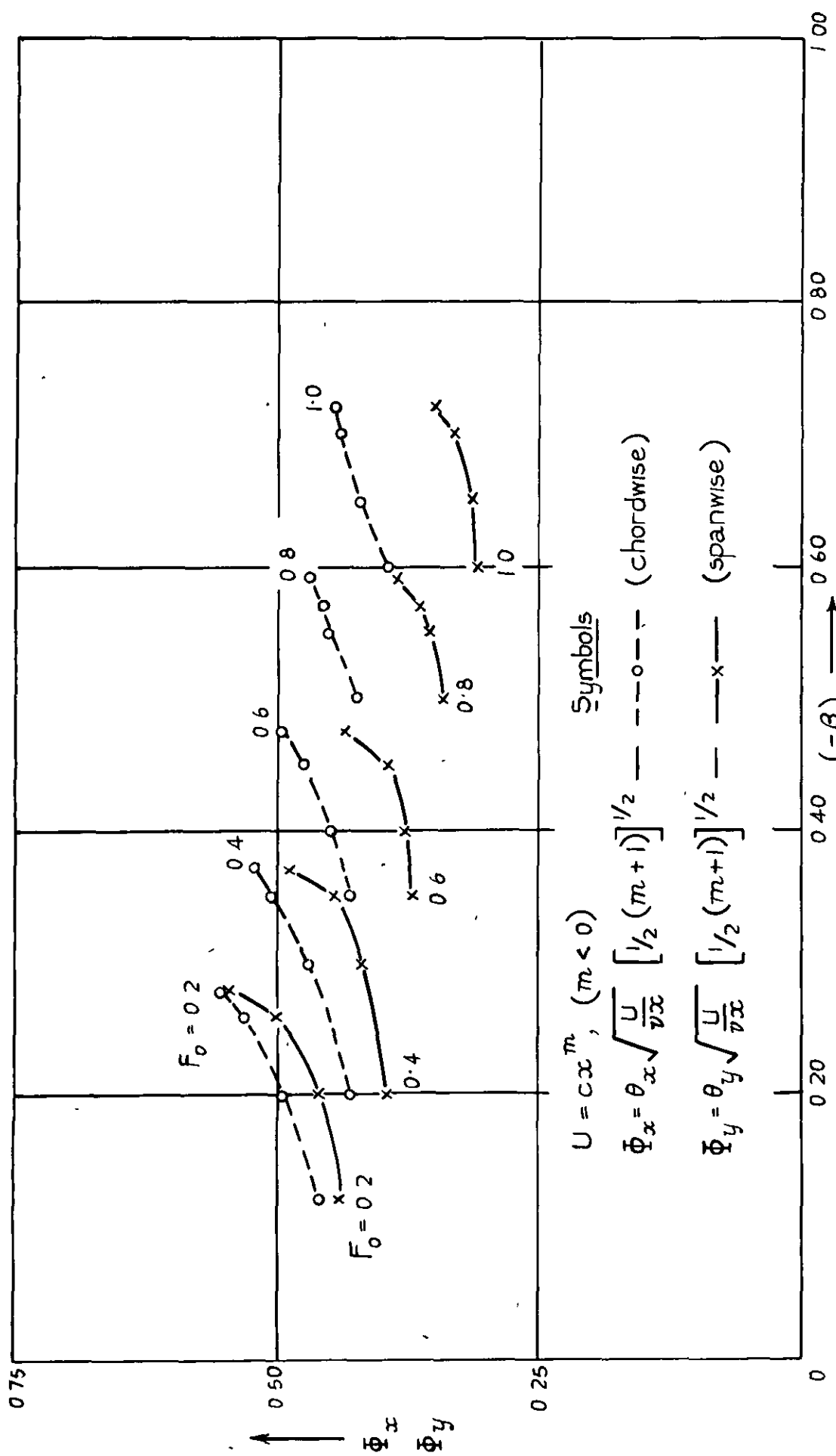

Variation of momentum thickness with K and β (negative)

FIG 16

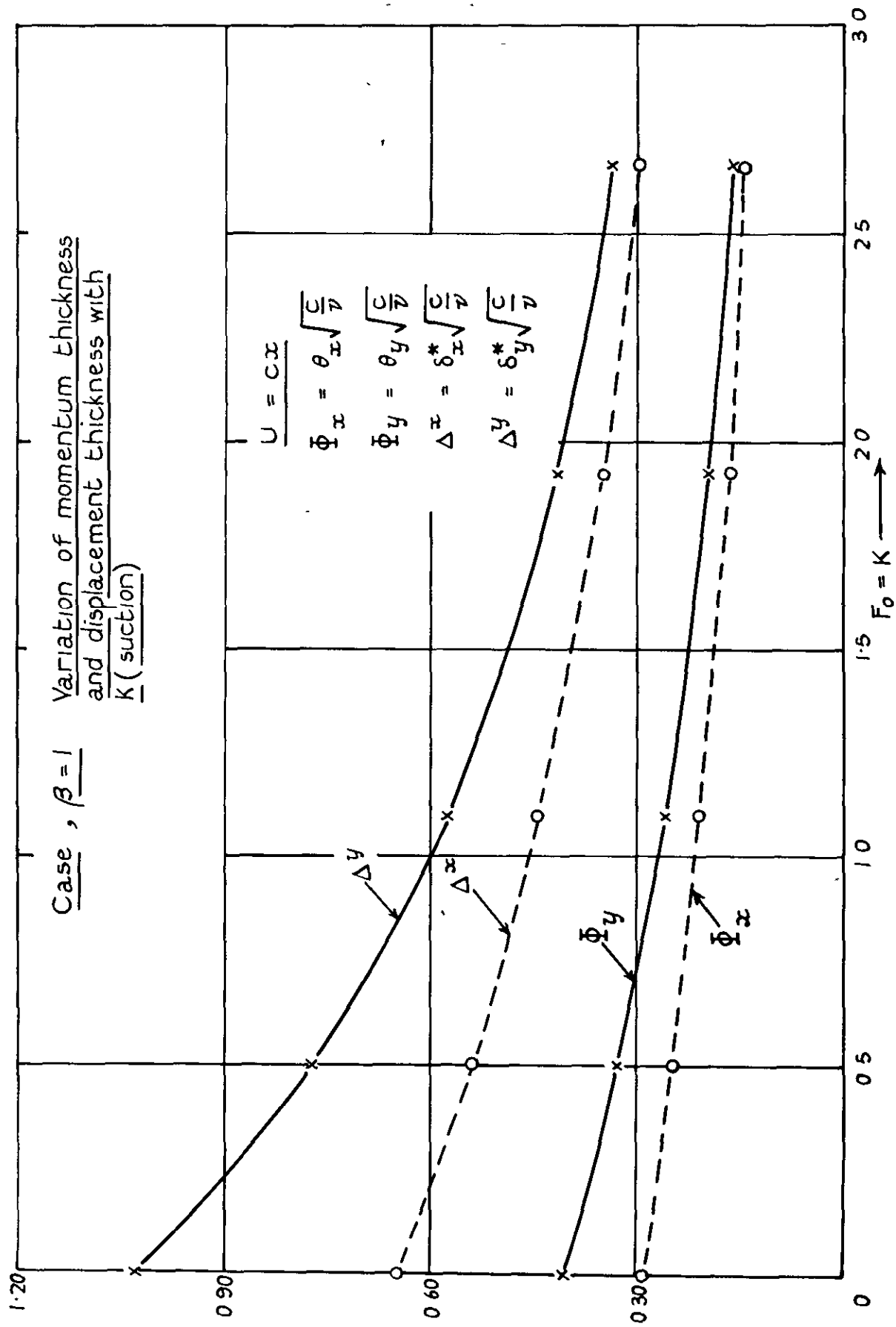
Case , β = 1
Variation of momentum thickness and displacement thickness with K (suction)
U = cx
$\Phi_x = \theta_x \sqrt{\frac{c}{\nu}}$
$\Phi_{hy} = \theta_{hy} \sqrt{\frac{c}{\nu}}$
$\Delta^* x = \Delta^* x \sqrt{\frac{c}{\nu}}$
$\Delta^* hy = \Delta^* hy \sqrt{\frac{c}{\nu}}$
Δ_{hy}
Δ_x
Φ_{hy}
Φ_x
1·20
0·90
0·60
0·30
0
0·5
1·0
1·5
2·0
2·5
3·0
$F_0 = K$

FIG 17

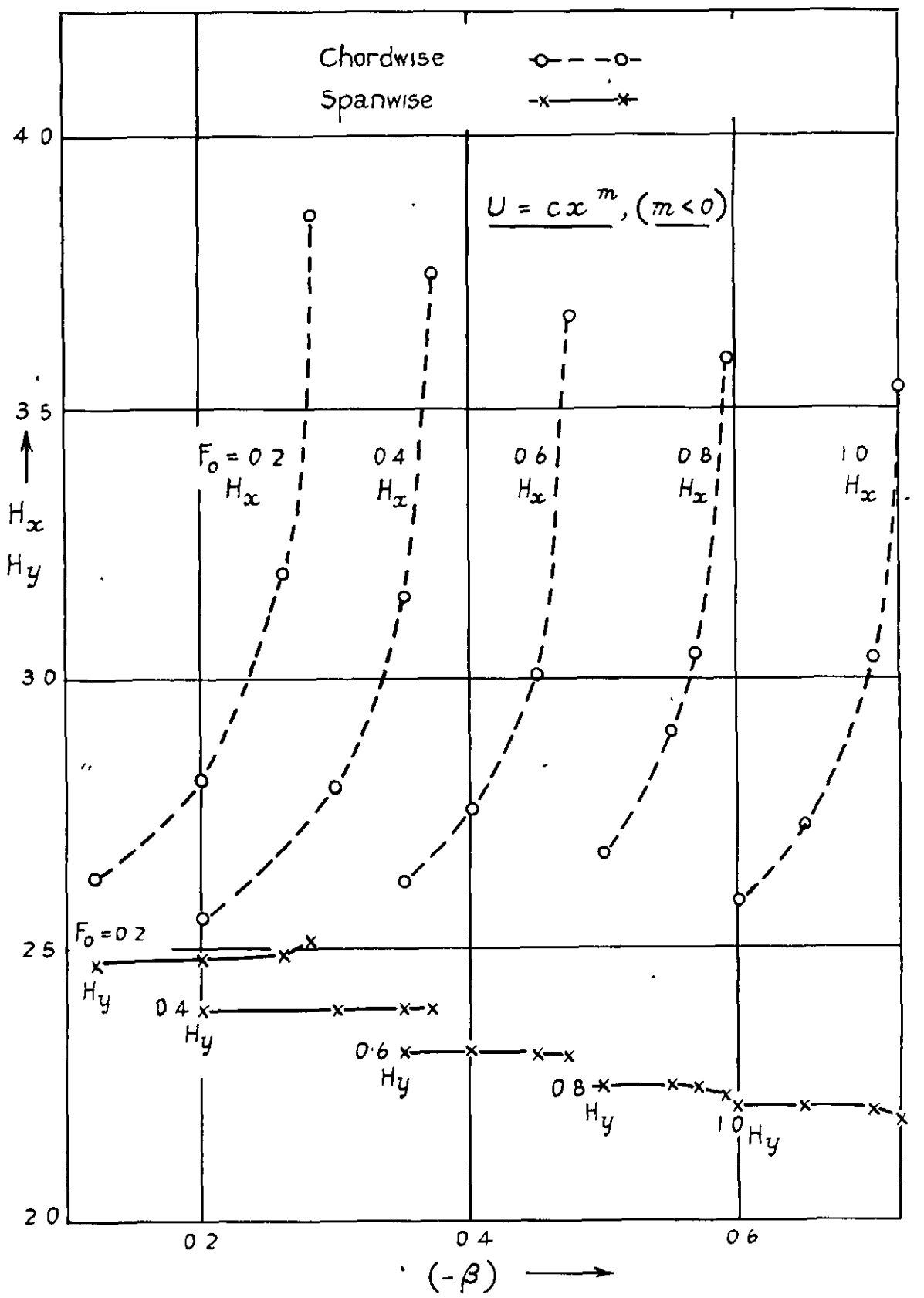

Variation of H with F_0 and β (negative)

FIG. 18.

Case $\beta = 1$ Variation of H with F_0

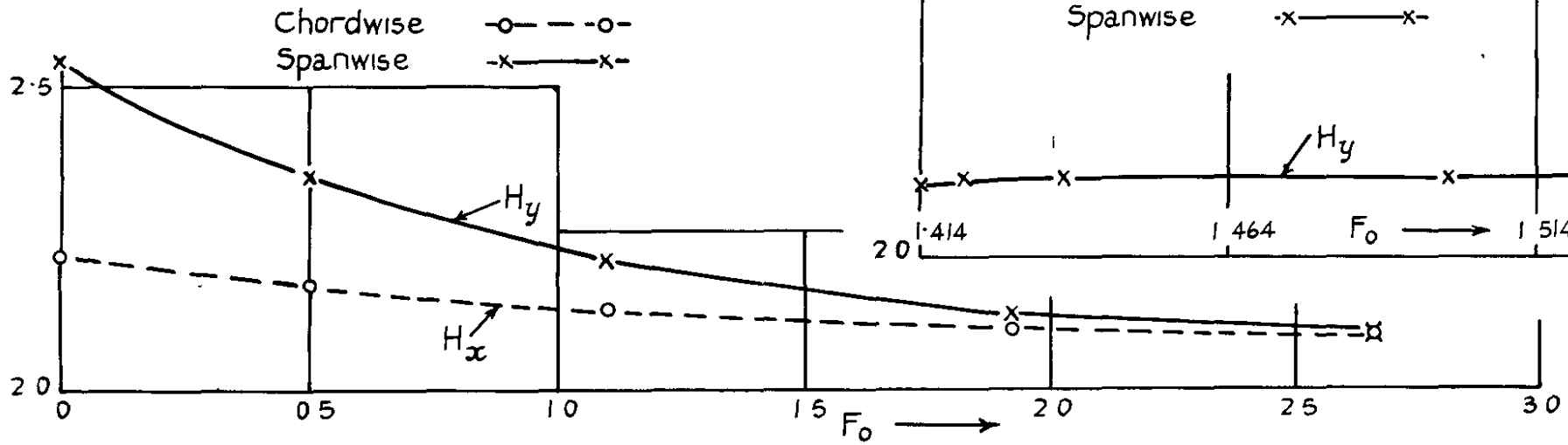

FIG 19.

Case $\beta = -1$, $U = cx^{-1/3}$

Variation of H with F_0

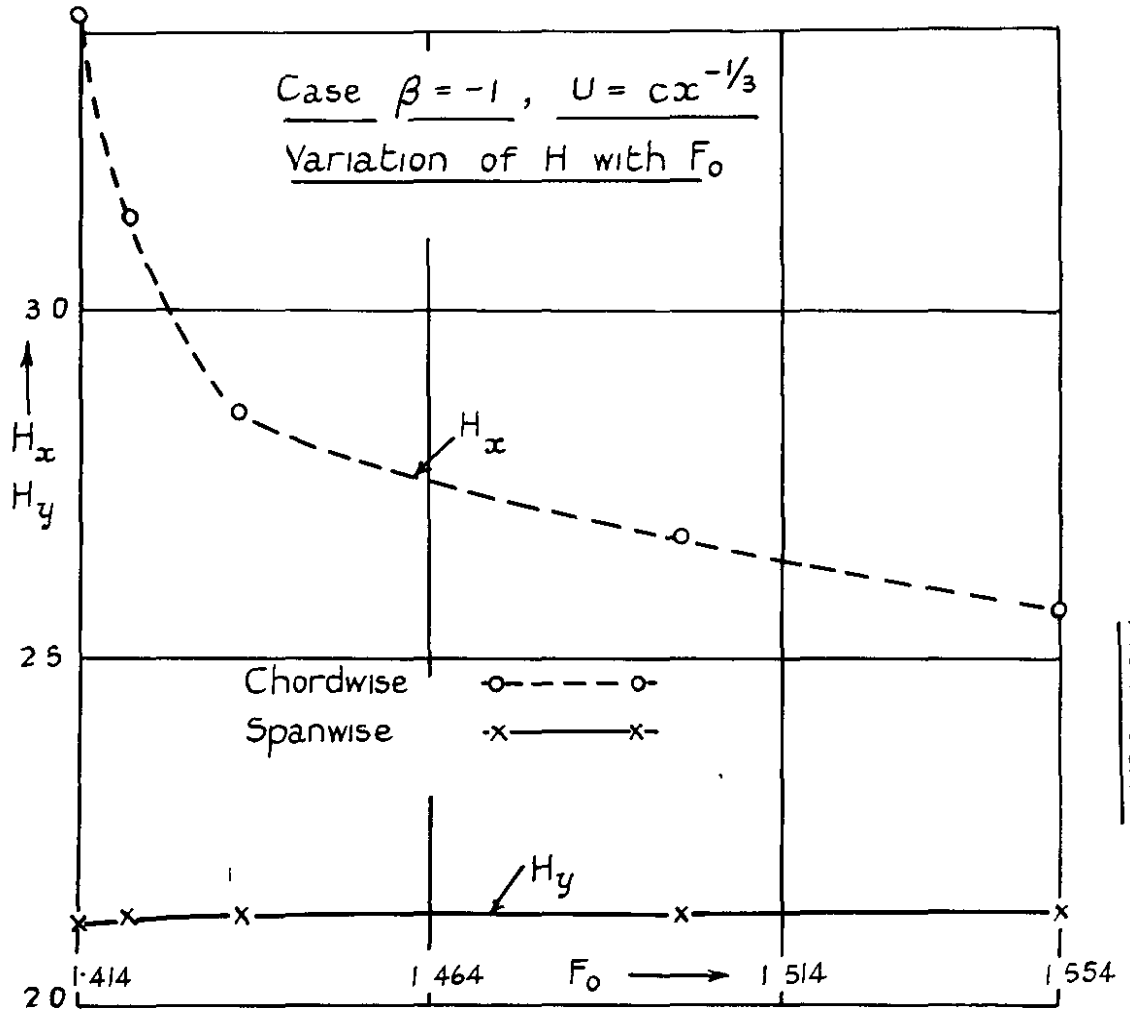

FIGS 18 & 19

Printed and published by
HER MAJESTY'S STATIONERY OFFICE

To be purchased from
York House, Kingsway, London W C.2
423 Oxford Street, London W.1
P.O. Box 569, London S E 1
13A Castle Street, Edinburgh 2
109 St. Mary Street, Cardiff
39 King Street, Manchester 2
Tower Lane, Bristol 1
2 Edmund Street, Birmingham 3
80 Chichester Street, Belfast
or through any bookseller

Printed in Great Britain

S O Code No 23-9009-14